ABSTRACT

Title of Document: New Concepts for Gelation of Alginate and its Derivatives
Vishal Javvaji, Doctor of Philosophy, 2013

Directed By: Professor Srinivasa R. Raghavan & Professor Gregory F. Payne

Bioengineering applications require materials that offer tunable and precise control over material properties. In particular, hydrogels of the polysaccharide, alginate have been widely studied for applications such as drug-delivery vehicles, matrices for encapsulation of cells, and scaffolds for tissue engineering. The ability of alginate to form a physically cross-linked hydrogel under mild conditions is a key factor for many applications. Traditionally, alginate gelation has been induced by the addition of divalent ions like calcium (Ca^{2+}). In this work, we explore new ways to induce gelation of alginate or its derivatives. These new routes are of interest because they can allow researchers to circumvent current limitations and moreover they can also enable new applications. Three new concepts are explored: (1) ionic gelation activated by light; (2) ionic gelation activated by an enzyme and its substrate; (3) gelation of hydrophobically modified alginate mediated by biological cells.

In our first study, we demonstrate a concept for ionic gelation of alginate in response to light, which enables us to create chemically erasable and spatially selective patterns of alginate gels. We impart light responsiveness by combining alginate, an insoluble calcium vector (e.g., $CaCO_3$) and a light responsive component, viz. a

photoacid generator (PAG). Upon UV irradiation, the PAG dissociates to release H^+ ions, which react with the $CaCO_3$ to generate free Ca^{2+} *in-situ*. In turn, the Ca^{2+} ions cross-link the alginate to form a gel. We show photopatterning of alginate gels, which are used to entrap contents (e.g., microparticles) and subsequently release them by a Ca^{2+} chelator.

In our second study, we demonstrate enzymatic gelation of alginate. Here, we use an enzyme/substrate reaction to generate H^+ ions. The components of our system are glucose oxidase (GOx, enzyme), glucose (substrate), alginate and $CaCO_3$. First, GOx catalyzes oxidation of glucose to generate H^+ ions. These H^+ ions solubilize $CaCO_3$ and release free Ca^{2+} ions *in-situ*. In turn, Ca^{2+} ions cross-link alginate chains into a gel. A sol-gel transition is observed only when GOx senses and catalyzes glucose. By exploiting the specificity of the enzyme for its substrate, we use this concept to build a visual test for the presence of glucose in an unknown product.

In our final study, we induce gels by combining a hydrophobically modified (hm) derivative of alginate with biological cells. Gelation occurs due to hydrophobic interactions between the grafted hydrophobes and the bilayers of biological cells. The polymer chains thus get attached to the cells and bridge the cells into a three-dimensional network. This gelation can also be reversed (to release the cells) by addition of a supramolecule, α-cyclodextrin, which has a hydrophobic binding pocket that binds to the hydrophobes. Cell gelation by hm-alginate may be useful in cell culture and tissue engineering applications. As a step towards these potential applications, we show that the process of gelation by hm-alginate is benign to the cells.

NEW CONCEPTS FOR GELATION OF ALGINATE AND ITS DERIVATIVES

By

Vishal Javvaji

Dissertation submitted to the Faculty of the Graduate School of the University of Maryland, College Park, in partial fulfillment of the requirements for the degree of

Doctor of Philosophy

2013

Advisory Committee:

Prof. Srinivasa Raghavan, Dept. of Chemical & Biomolecular Engineering, Advisor
Prof. Gregory F. Payne, Fischell Dept. of Bioengineering & IBBR, Co-Advisor
Prof. Panagiotis Dimitrakopoulos, Dept. of Chemical & Biomolecular Engineering
Prof. Ganesh Sriram, Dept. of Chemical & Biomolecular Engineering
Prof. Ian M. White, Fischell Dept. of Bioengineering

Dedication

This dissertation is dedicated to my parents and my family for teaching me the value of education, for their encouragement and for their unconditional love and support.

Acknowledgements

First and foremost, I would like to thank my advisors Prof. Srinivasa Raghavan and Prof. Gregory Payne for providing me the opportunity to be a part of their groups and for providing continuous guidance, encouragement and support. Their mentoring had a very significant role in shaping up of not only my scientific career but also on my approach to different aspects of life. I feel extremely lucky for having numerous fruitful interactions with them from which I have incrementally learnt a lot. Before coming to Maryland, I heard so many horror stories about life in grad school, but on the contrary, I enjoyed my grad school (mostly possible because of my advisors).

Next, I owe a lot of thanks to my family for their unconditional love and support. Particularly, I am extremely grateful to my parents, Madhu and Shylaja. They taught me the importance of education and supported me throughout my school. Also, I would like to thank my brother (Vivek) and my aunt (Jyothi). I would also like to acknowledge Tripura and other friends - Yugandhar, Lalith and Syamal for all the support.

I would like to thank my committee members: Prof. Ganesh Sriram, Prof. Panagiotis Dimitrakopoulos, Prof. Ian white for their invaluable guidance, suggestions and input for my projects.

I owe a lot of thanks my present and past colleagues from Dr. Raghavan's lab and Dr. Payne's lab. I was fortunate to be a part of such an enthusiastic, intellectual and productive groups. It has been a great pleasure to interact with them.

TABLE OF CONTENTS

LIST OF FIGURES

Chapter 1

INTRODUCTION AND OVERVIEW

1.1. PROBLEM DESCRIPTION AND MOTIVATION

Biomedical and bioengineering applications require materials that offer tunable and precise control over material properties.[4-6] An important class of materials in such applications are hydrogels, which are connected networks of polymer chains that are swollen with water. Hydrogels of naturally occurring biopolymers, such as proteins and polysaccharides, are particularly attractive due to their nontoxicity and biocompatibility. Among the polysaccharides, sodium alginate, an anionic polysaccharide derived from brown algae, has emerged as a material of choice for creating hydrogels, especially for cell encapsulation and tissue engineering.[5] This polymer and its gelation, i.e., conversion from a liquid state to a gel state, will be the focus of this dissertation.

Because of the tremendous interest in alginate as a biomaterial, there has been considerable effort into elucidating new routes for alginate gelation. Conventionally, alginate hydrogels are formed by addition of a soluble calcium salt to alginate solutions. The Ca^{2+} ions serve to connect or cross-link adjacent linear chains of alginate in water and thereby generate a cross-linked hydrogel. However, the addition of Ca^{2+} ions directly to the polymer solution creates an inhomogenous gel structure.[7] To overcome the problem of inhomogeneity, alginate gelation has been carried out using *in situ* generated Ca^{2+} ions. This method uses the time-dependent hydrolysis of glucono-δ-lactone (GDL)

to generate gluconic acid, which in turn reacts with insoluble calcium carbonate ($CaCO_3$) particles to generate free Ca^{2+}.[7] Gelation via GDL has been shown to give rise to more homogenous alginate gels.

While alginate gelation can be induced by Ca^{2+}, many researchers have sought to find unconventional ways to accomplish the same. For example, alginate gelation has been reported to occur under the action of external stimuli like light,[8,9] electricity,[10,11] and temperature[12] or even with uncommon chemical inputs (e.g., enzymes or substrates). Extending the gelation phenomena to these new routes often imparts unique properties and applications to these gels (for example, light-induced gelation can be made to occur in a spatially selective manner). Gelation of a chemically modified derivative of alginate has also been made to occur upon activation of an enzymatic reaction[13] or in conjunction with biological cells.[14] Most of the above examples of alginate gelation have involved rather complex steps, e.g., complicated synthesis schemes to generate stimuli-responsive alginate derivatives or photoresponsive molecules.

The aim of this dissertation is to explore new or uncommon concepts for gelation of alginate and its derivatives. Our focus is on relatively simple approaches that avoid labor-intensive chemical synthesis and can be conducted with inexpensive chemicals and materials that are readily available. Simple approaches have the advantage that they can be easily used (and adapted) by other researchers or even scaled-up for commercial use.

1.2. PROPOSED APPROACH

In this dissertation, we will demonstrate three new concepts for alginate gelation, as described below.

1.2.1. Light-Activated Ionic Gelation of Alginate

In Chapter 3, we demonstrate a new and simple concept for ionic gelation of alginate in response to light. Our approach involves combining an insoluble salt of calcium (e.g., calcium carbonate, $CaCO_3$) with an aqueous solution of sodium alginate along with a third component, a photoacid generator (PAG). Upon UV irradiation, the PAG dissociates to release H^+ ions, which react with the $CaCO_3$ to generate free Ca^{2+}. In turn, the Ca^{2+} ions cross-link the alginate chains into a physical network, thereby resulting in a hydrogel. As a step toward potential applications, we show the ability to photopattern a thin film of alginate gel onto a glass substrate under mild conditions.

1.2.2 Enzymatic Gelation of Alginate

In Chapter 4, we present a new concept by which ionic gelation of alginate occurs in response to the addition of an enzyme and its substrate. Similar to the light-responsive alginate mentioned above, this approach also involves combining an insoluble salt of calcium ($CaCO_3$) with an aqueous solution of sodium alginate. The additional components here are the enzyme, glucose oxidase (GOx) and its small-molecule substrate glucose. Addition of glucose to alginate/$CaCO_3$/GOx triggers a cascade reaction which leads to gel formation. First, glucose gets oxidized by GOx to generate gluconic acid, which then releases H^+ ions. Next, the H^+ ions react with $CaCO_3$ to generate free Ca^{2+}

ions *in situ*. These Ca^{2+} ions crosslink alginate chains to form a Ca-alginate gel. A notable aspect of this enzymatic gelation scheme is that gelation of alginate is very specific: i.e., it occurs only when the right substrate (glucose) is added, but not upon addition of analogous small molecules like fructose or sucrose.

1.2.3. Cell-mediated Gelation of an Alginate Derivative

In Chapter 5, we describe gelation of an alginate derivative in conjunction with biological cells. The derivative used in this context is hydrophobically modified (hm) alginate, formed by grafting alkyl tails (hydrophobes) to the backbone of the polymer. We show that hm-alginate gels a variety of biological cells (blood, cancer cells, endothelial cells). Gelation occurs because of hydrophobic interaction between the grafted hydrophobes and the hydrophobic lipid membrane of biological cells. The polymer chains thus get attached to the cells and bridge the cells into a three-dimensional network. This gelation can also be reversed (to release the cells) by addition of a supramolecule, α-cyclodextrin, which has a binding pocket that binds to the hydrophobes.

1.3. SIGNIFICANCE OF THIS WORK

The studies described in this dissertation are potentially significant from both scientific and practical standpoints. From a scientific point of view, the light-activated alginate gelation method in Chapter 3 offers a route to build spatial patterns of soft materials by combining the principles of triggered self-assembly and photolithography. This approach can be extended to other biopolymers such as pectin. Inspired by this study, other researchers have also extended the same approach to light-activated gelation

of peptides.[15] Regarding the enzymatic gelation of alginate (Chapter 4), the significance of this approach lies in the fact that it couples the specificity of enzymes to their substrate with an unrelated macroscopic assembly process (gelation). Alginate gelation can be caused by a variety of divalent or trivalent cations in addition to Ca^{2+}, i.e., it is not very specific. However, the GOx enzyme acts only on glucose and not on similar molecules like fructose and we are able to impart this specificity to the gelation process. Lastly, our study in Chapter 5 offers a simple and benign way to connect cells into a polymer-bridged network structure while still remaining viable. We believe this is a step towards the bottom-up assembly of cell clusters and tissue. Gels of cancer cells may also serve as a platform to test and discover new anti-cancer drugs.

The three above studies also could prove to be useful for specific applications. Light-responsive alginate gelation may be useful in the creation of new biomedical devices or biosensors. Spatially patterned gels may be employed in combinatorial studies for drug discovery. Enzymatic gelation of alginate is directly applicable as a simple way to test for the presence of glucose in food products. Finally, the use of hm-alginate to gel blood cells has immediate utility in the treatment of severe bleeding injuries, i.e., this polymer can serve as a hemostatic material for use by the military, emergency responders, and trauma surgeons. In addition, gels of hm-alginate and cells could be potentially applicable as injectable biomaterials. Overall, our research will help to increase the importance and utility of alginate as a biomaterial.

Chapter 2

BACKGROUND

This dissertation is focusses on gelation of alginate and its derivatives in response to different stimuli. In this chapter, we begin with a brief introduction to alginate and its properties. We then switch to the introductions of other important components of the gelation systems which are presented in Chapter 3, 4 and 5. In particular, we briefly describe background about photoacid generators, glucose oxidase, hydrophobically modified alginate and cyclodextrins. After that, we describe the techniques that we used to study the gelation system, such as rheology and microscopy.

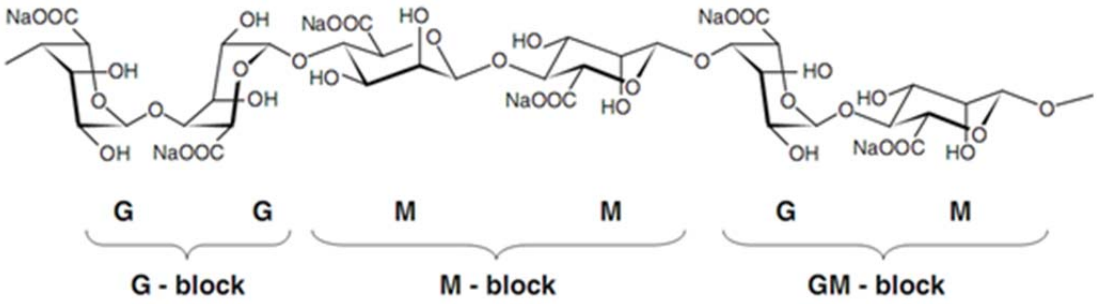

Figure 2.1. Chemical structure of sodium alginate

2.1. ALGINATE

Sodium alginate, an anionic polysaccharide derived from brown algae, is a linear unbranched polymer containing blocks of 1,4-linked β-D-mannuronic (M) and α-L-guluronic (G) residues. It is a block copolymer comprised of sequences of M blocks, G-

blocks and some interspersed MG blocks.[16]. Figure 2.1 shows a representative chemical structure of alginate. In water, sodium alginate forms low-viscosity solutions (sols)

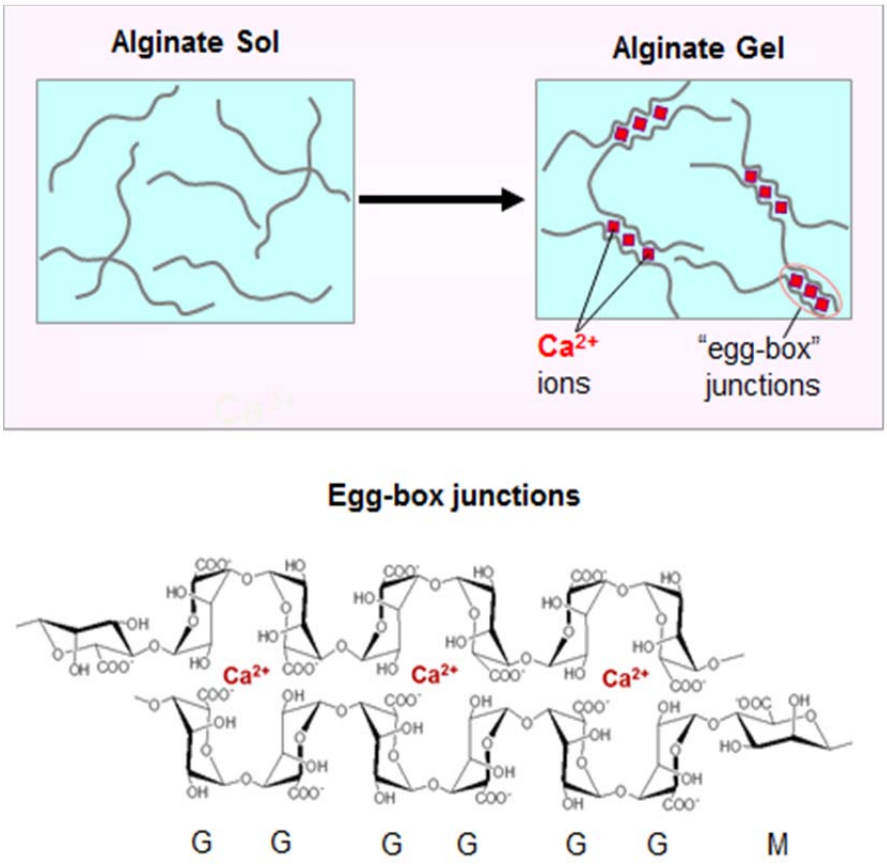

Figure 2.2. (a) Schematic illustration showing sol-gel transition of alginate upon addition of calcium ions. (b) Proposed structure of "egg-box" junctions in ca-alginate gel.

These sols can be converted to physical hydrogels by ionic crosslinking with multivalent cations (like Ca^{2+}, Ba^{2+}, Al^{3+}, etc).[6] As shown by Figure 2.2, Ca^{2+} ions electrostatically bind to the carboxylic acid groups in the G-blocks of adjacent alginate chains. This creates domains where the Ca^{2+} ions are sequestered within the G blocks like eggs in an egg-box; as a result these zones are called "egg-box" junctions.[17,18] When such junctions pervade the volume, the alginate chains are connected into a volume-filling three-dimensional network and thus an elastic hydrogel is formed. An advantage of these

ionically cross-linked gels is that they can be reversed (or ungelled) under mild conditions. Upon addition of calcium chelators (e.g., sodium citrate) to Ca-alginate gels, they preferentially bind to calcium ions and thereby disrupting the cross-links between the alginate polymers which causes its un-gelation.

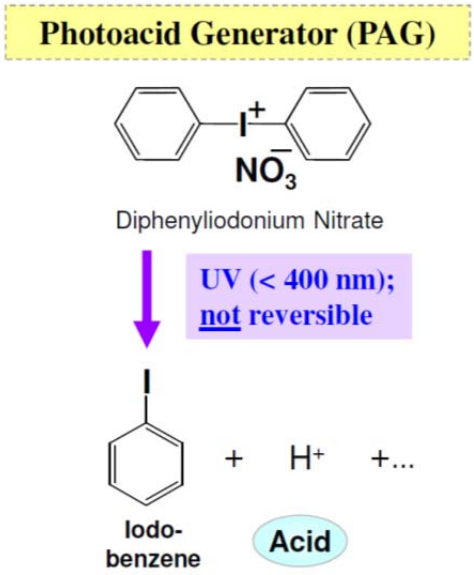

Figure 2.3. Mechanism of acid generation by photolysis of diphenyliodonum nitrate. Upon UV irradiation, diphenyliodonium nitrate forms a mixture of hydrophobic byproducts (including Iodobenzene) and generates H^+ ions which causes a pH decrease in the reaction mixture.

2. 2. PHOTOACID GENERATORS

Photoacids generators (PAG) are class of molecules which generate acid moieties in response to light. They have been extensively used in cationic polymerizations and photolithographic applications.[19] Broadly, these ionic photoacid generators can be classified into diaryliodonium salts and triarylsulfonium salts with different substituent groups and counter ion combinations. Few notable examples are: diphenyliodonium

nitrate, diphenyliodonium p-toluenesulfonate, diphenyliodonium hexafluorophosphate, triphenylsulfonium triflate

Although there are various commercially available products, the important factors that determine a PAG's successful use in an application are its solubility, amount of acid generated and its wavelength sensitivity. In the current study, we used a cationoic photoacid generator, diphenyliodonium nitrate which is commercially available from Sigma and is relatively inexpensive. It has its primary absorption peak at 203 nm and secondary absorption peak at 226 nm. Upon UV irradiation, diphynliodonium nitrate dissociates into a mixture of hydrophpobic compounds (including iodobenzene, 2-,3-,4-iodobiphenyls, biphenyls) and acid moieties (H^+).[19] Figure 2.3 shows a mechanism for ultraviolet light induced acid generation of diphenyliodonium nitrate.

2. 3. GLUCOSE OXIDASE

Glucose oxidase is an oxidoreductase enzyme that catalyzes oxidation of β-D-glucose to gluconic acid and hydrogen peroxide by using molecular oxygen as a co-substrate.[20] The molecular weight of GOx ranges between 130-170 kDa.[20] It is widely used in food applications, sensing applications (glucose detection kits) and biopharmaceutical applications.[20]

2.4. HYDROPHOBICALLY MODIFIED ALGINATE

Hydrophobically modified alginate (hm-alginate) was synthesized by addition of hydrophobic moieties to the hydrophilic alginate backbone. In this particular study, we focused on attaching surfactant (octylamine) based hydrophobic molecules to alginate backbone. Based on previously reported studies, hm-alginate can be synthesized by three different reaction procedures: (i) using sodium periodate. (ii) using tertiary butyl alchohol (TBA) and (iii) using 1-Ethyl-3-(3-dimethylaminopropyl)carbodiimide (EDC).

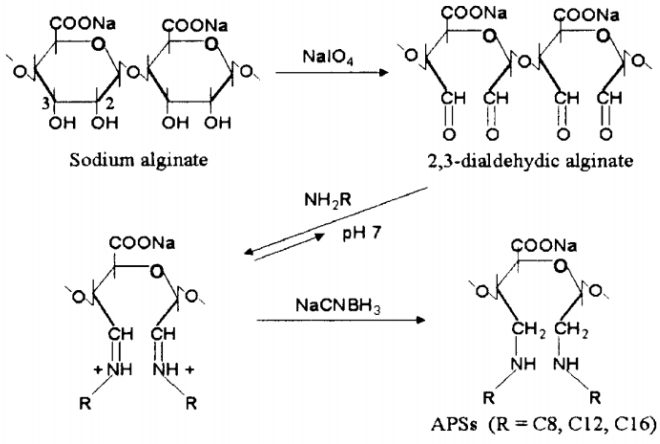

Figure 2.4. Reaction scheme (adapted from Yang et al.[1]) for synthesis of hm-alginate using sodium periodate.

Yang et al.[1] reported hm-alginate synthesis using sodium periodate. Figure 2.4 shows reaction mechanism to synthesize alkyl hydrophobe grafted hm-alginate. Briefly, aqueous solution of alginate was reacted with sodium periodate to generate reactive dialdehyde groups on alginate backbone. Oxidized alginate is then reacted with octylaamine (or other amine ending hydrophobe) followed by subsequent reduction of C=N bond using sodium cyanoborohydride and filtered to obtain hm-alginate. A disadvantage with this mechanism is that initial oxidation with sodium periodate also causes chain scission which leads to a dramatic decrease in molecular weight.

Eslaminejad et al.[3] reported synthesis of hm-alginate using TBA. Figure 2.5 shows scheme of reactions for preparation of C18 hydrophobe grafted alginate. Briefly, sodium ions were first replaced with TBA (first by neutralization with sodium hydroxide followed by reaction with TBA). TBA substituted alginate was lyophilized, redissolved in DMSO and then reacted with alky bromide hydrophobe to graft alkyl hydrophobes on alginate. After the grafting reaction, remaining TBA ions were replaced with sodium ions and then purified to get do hydrophobically modified alginate.

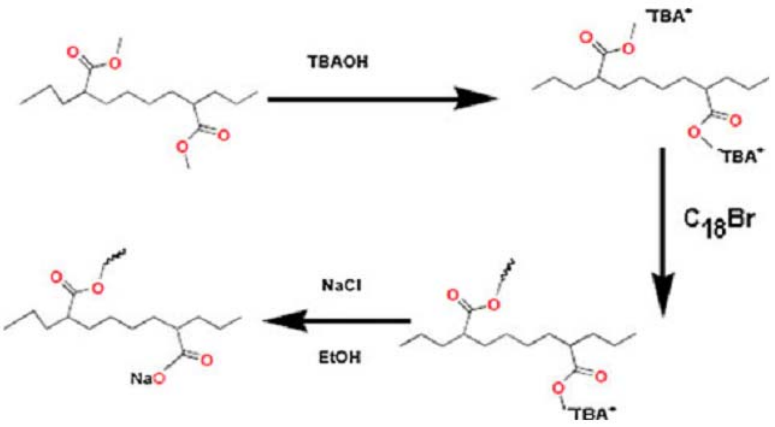

Figure 2.5. Reaction scheme (adapted from Eslaminejad et al.[3]) for synthesis of hm-alginate using tertiary butyl alchohol.

Nystrom et al.[2] reported synthesis of hm-alginate using EDC. Figure 2.6 shows reaction scheme for synthesizing hm-alginate using EDC. Briefly, aqueous solutions of alginate are acidified using hydrochloric acid to a pH around 3.4 and then EDC is added to the reaction mixture. EDC reacts (and activates) carboxylic acid groups on the alginate to form o-Acylisourea based intermediate which then quickly reacts with amine groups of the hydrophobe to form a hm-alginate with stabile amide bond between alginate and the hydrophobe. Acetone is added to the reaction mixture to precipitate hm-alginate.

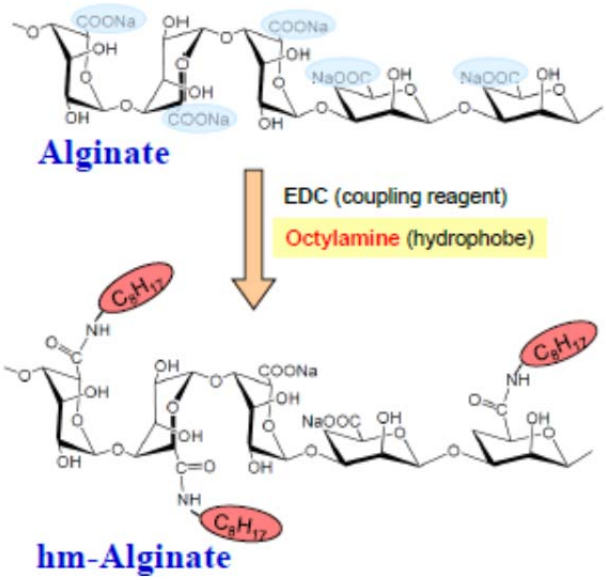

Figure 2.6. Reaction scheme for synthesis of hm-alginate using EDC.

2. 5. CYCLODEXTRINS

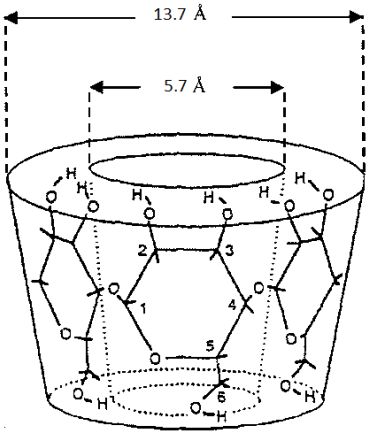

Figure 2.7. Truncated cone-shaped conformation of α-Cyclodextrin.[2]

Cyclodextrins (CDs) are cyclic oligosaccharides containing D-(+) glucopyranose units attached by α-(1,4) glucosidic bonds, as shown in Figure 2.7.[21] They are rigid, truncated cone-shaped structures, with an internal cavity of size 5 to 8 Å depending upon the number of glucopyranose units. The wide side of the truncated cone is bordered by the secondary hydroxyl groups (2-OH and 3-OH), while the primary hydroxyl groups (6-OH) are on the narrow side. The molecule is stiffened by hydrogen bonding between the 2-OH and 3-OH groups around its outer rim. Note that all hydroxyl groups are located on the outside of the molecular cavity, thereby making the outer surface hydrophilic. On the other hand, no hydroxyl groups are located in the inner cavity, which is thus hydrophobic. CDs thus have hydrophilic outer surfaces and hydrophobic inner cavities. Because of their unique structure, CDs can form host-guest inclusion complexes with various hydrophobic guest molecules or hydrophobic parts of these molecules.[22-26] Note that the bonding between the CD and the guest is through non-covalent interactions. In

chapter 5, we will be using α-CD (which has six glucose units) to sequester hydrophobes on hm-alginate chains.

2.6. CHARACTERIZATION TECHNIQUE – I: RHEOLOGY

Rheology is formally defined as the study of flow and deformation in materials.[27] Rheological measurements provide important information on soft materials, specifically on the relation between microstructure and macroscopic properties. These measurements are typically performed under steady or dynamic shear. In steady shear, the sample is subjected to a constant shear-rate $\dot{\gamma}$ (e.g. by applying a continuous rotation at a fixed rate on a rotational instrument), and the response is measured as a shear-stress σ. The ratio of shear-stress σ to shear-rate $\dot{\gamma}$ is the (apparent) viscosity η. A plot of the viscosity vs. shear-rate $\dot{\gamma}$ is called the flow curve of the material.

Rheological experiments can also be conducted in dynamic or oscillatory shear, where a sinusoidal strain $\gamma = \gamma_0 \sin(\omega t)$ is applied to the sample. Here γ_0 is the strain-amplitude (i.e. the maximum applied deformation) and ω is the frequency of the oscillations. The sample response will be in the form of a sinusoidal stress $\sigma = \sigma_0 \sin(\omega t + \delta)$ which will be shifted by a phase angle δ with respect to the strain waveform. Using trigonometric identities, the stress waveform can be decomposed into two components, one in-phase with the strain and the other out-of-phase by 90°:

$$\sigma = G'\gamma_0 \sin(\omega t) + G''\gamma_0 \cos(\omega t)$$

where G' is the **Elastic** or **Storage Modulus** and G'' is the **Viscous** or **Loss Modulus**.

The physical interpretations of the two moduli are as follows. The elastic modulus G' is the in-phase component of the stress and provides information about the elastic nature of the material. Since elastic behavior implies the storage of deformational energy, this parameter is also called the storage modulus. The viscous modulus G'', on the other hand, is the out-of-phase component of the stress and characterizes the viscous nature of the material. Since viscous deformation results in the dissipation of energy, G'' is also called the loss modulus. For these properties to be meaningful, the dynamic rheological measurements must be made in the "*linear viscoelastic*" (LVE) regime of the sample. This means that the stress must be linearly proportional to the imposed strain (i.e., moduli independent of strain amplitude). In that case, the elastic and viscous moduli are only functions of the frequency of oscillations ω, and are true material functions. A log-log plot of the moduli vs. frequency, i.e. $G'(\omega)$ and $G''(\omega)$, is called the frequency spectrum of the material and represents a signature of the material microstructure.

The important advantage of dynamic shear is that it allows us to characterize microstructures without disrupting them in the process. The net deformation imposed on the sample is minimal because the experiments are restricted to small strain amplitudes within the LVE regime of the sample. As a result, the linear viscoelastic moduli reflect the microstructures present in the sample at rest. This is to be contrasted with steady shear, where the material functions are always obtained under flow conditions corresponding to relatively drastic deformations. We can therefore correlate dynamic

rheological parameters to static microstructures, and parameters under steady shear to flow-induced changes in microstructure.

2.7. CHARACTERIZATION TECHNIQUE – II: OPTICAL MICROSCOPY

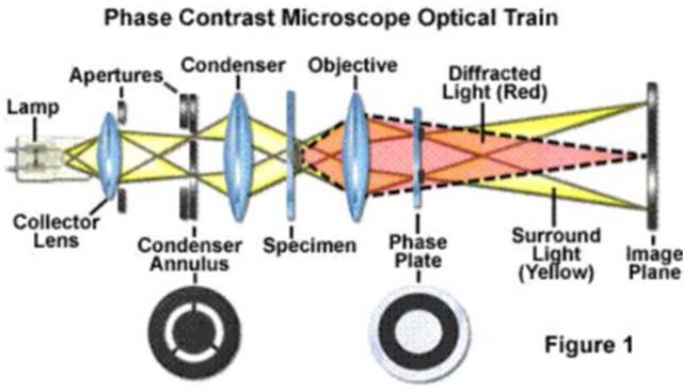

Figure 2.8. Schematic representation of light path in phase contrast microscopy (from www.microscopy.com)

Phase-contrast microscopy, a technique frequently used to image cells, utilizes the relationship between diffracted light from the sample and undiffracted background light. [28,29] In general, when light passes through an object, it is slowed down by ¼ of a wavelength in comparison with the undiffracted background light. However, ½ of a wavelength phase shift is needed in order to produce destructive interference that result in contrasting imaging. Based on this concept, the main components of a phase contrast microscope consist of an annular ring in the condenser and a phase plate in the back focal plane of the objective to achieve the required phase shift (Figure 2.8). The annular ring controls where the undiffracted background light will go. Undiffracted light, after passing through the plane of the sample, will focus on the back focal plane of the objective where it encounters the phase plate. The phase plate is modified to allow this light to travel through with a ¼ wavelength jump relative to the diffracted light from the sample. The resulting two ¼ wavelength differences (¼ wavelength for sample diffraction and ¼ from

phase plate) is combined to produce ½ of a wavelength phase shift to produce the contrasting image

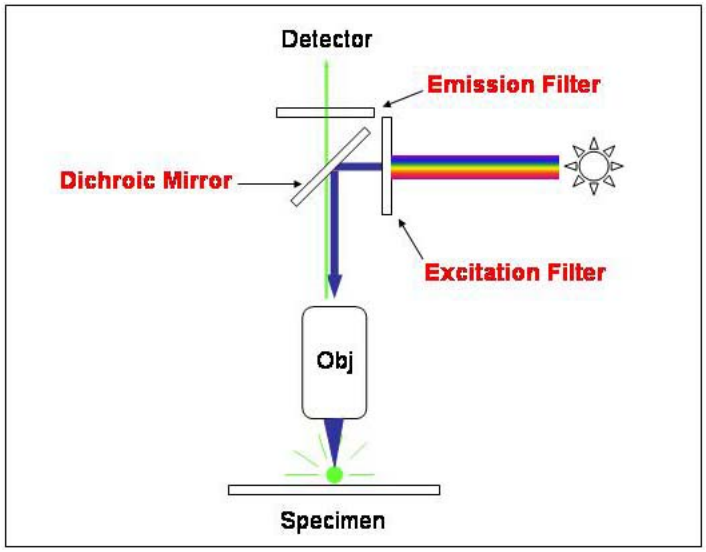

Figure 2.9. Schematic representation of light path in fluorescence microscopy (from http://en.wikipedia.org/wiki/Fluorescence_microscopy)

Fluorescence microscopy is another technique used in cell measurements.[29] In this work, we will use reflected-light fluorescence microscopy to image fluorescent particles embedded in alginate gels. As shown in Figure 2.9, the basic components of fluorescence microscope consist of a light source, a dichromatic light splitter, objective, and the detector. Excitation light, with short wavelength and high energy, is reflected by the dichromatic beam splitter through the objective and onto the sample. Upon excitation, the sample emits fluorescence in a lower energy wavelength which is then collected by the objective, passes through the dichromatic mirror and is imaged by detector.

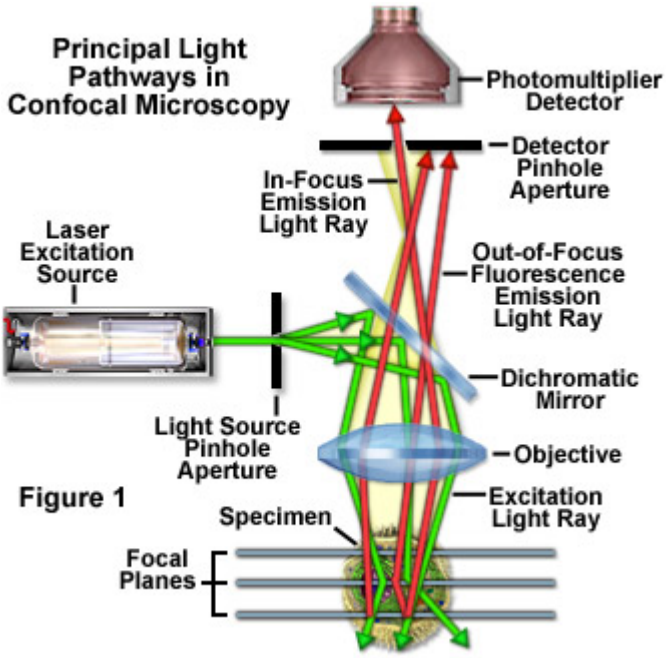

Figure 2.10. Schematic representation of light path in confocal fluorescence microscopy (from www.microscopyu.com)

We also used confocal microscopy in chapter 5 to image fluorescently labeled cells present in a 3D matrix. Confocal microscope is built on the concepts of fluorescent microscopes but has additional advantages in terms of eliminating out-of focus glare, ability to image thin optical slices of samples (for 3D reconstruction of objects). As shown in Figure 2.10, confocal microscope uses point illumination and a spatial pinhole (near the detector). By using this configuration it eliminates out of focus lights and detects light produced very close to the its focal planes. Imaging multiple focal planes allows us to reconstruct 3D structures of optical section of specimens.

Chapter 3

LIGHT-ACTIVATED IONIC GELATION OF ALGINATE

The results presented in this chapter have been published in the following journal article: Vishal Javvaji, Aditya G. Baradwaj, Gregory F. Payne, and Srinivasa R. Raghavan, "Light-activated ionic gelation of common biopolymers." *Langmuir*, 27, 12591-12596 (2011).

3.1. INTRODUCTION

The use of light as an external stimulus for tuning material properties is being actively investigated by engineers and scientists.[30-35] Compared to other stimuli such as temperature or electric fields, light offers significant advantages in that it can be directed precisely at a location of interest with micron-scale resolution and from a distance (i.e., avoiding direct contact). Accordingly, numerous researchers have been seeking to impart photoresponse to materials so that the properties of the material can be tuned by light. In the context of self-assembly, which involves weak, non-covalent interactions, there have been many attempts at creating assemblies that can be switched from one morphology to another using light. For example, light-responsive self-assembly has been used as the basis for photorheological (PR) fluids,[36] which are fluids whose rheological properties can be tuned by light. One example is a system that undergoes a light-induced sol-to-gel (fluid-to-solid) transition due to the light-induced assembly of individual molecules into a nanofibrous network.[32-34] Such self-assembly-based gelation is distinct from UV-activated crosslinking (free-radical polymerization). Specifically, self-assembled gels are

weak networks that can be subsequently liquefied either by irradiation with a different wavelength of light or by changes in temperature, pH or composition.[32-34]

Our lab has recently become interested in imparting photoresponse to assemblies such as micelles,[37,38] reverse micelles,[39] and nanoparticle networks[40]. While most previous work in this area focused on designing novel photoresponsive molecules (such as azobenzene-modified surfactants[31,41] or molecular gelators[32-34]), we have focused on finding simpler routes to photoresponsive systems that involve no chemical synthesis, i.e., the materials can be prepared by mixing commercially available entities. For example, we have created photoresponsive micelles by doping common surfactants with a cinnamic acid derivative.[37,38] In another study, we developed a photoresponsive aqueous dispersion of clay nanoparticles that transformed from sol to gel upon UV irradiation.[40] The concept in this case was to combine the nanoparticles with an amphiphilic stabilizer and a photoacid generator (PAG). PAGs are commercially available molecules that have been used for a long time in the microelectronics industry.[42-45] Their distinctive property is that they get photolyzed by UV light to form an acidic moiety.[42-45] In our system, the photolysis of the PAG caused the pH to drop by about 3 units, and in turn, the charges on the edges of the clay nanoparticles switched from negative to positive.[40] This charge reversal drove the initially separated particles to cluster into a gel network.[40]

In this study, we show how to impart photoresponsive properties to solutions of biopolymers. We again use a PAG as the photoactive component of the system. The

biopolymers employed here are sodium alginate and pectin, and the property shared by these is that their solutions undergo gelation in the presence of multivalent cations like Ca^{2+}, Ba^{2+} or Al^{3+}.[6,17,46] Alginate, in particular, is a popular biopolymer that is extensively used for encapsulating biological cells and for other biomedical applications.[6,7] For such applications, it would be advantageous to have an alginate formulation that could be crosslinked by light rather than by addition of ions. Indeed, two research groups have recently explored this very idea.[8,9] One group synthesized a derivative of alginate modified with methacrylate groups, and this polymer was covalently crosslinked into a gel by a free-radical mechanism.[8] A second group utilized a light-sensitive caged-calcium compound, which upon UV irradiation released Ca^{2+} ions that crosslinked alginate into a gel.[9] These approaches required either additional chemical synthesis steps or the use of expensive molecules such as the caged calcium, which impedes their large-scale applicability. For example, while the latter method was suitable for use with small amounts of material in a microfluidic device, the authors noted that it was unsuitable for creating bulk gels.[9] Also, with regard to covalently crosslinked alginate, one issue is that those gels cannot be liquefied (reversed) by addition of sodium citrate or other calcium chelators. The reversibility is a useful property because it permits the release from the gel of entrapped species such as cells or nanoparticles.

Here, we report a simple photogelation scheme using relatively inexpensive, commercially available components that can be used to create bulk gels and films of alginate and other biopolymers. The gels are physically (non-covalently) crosslinked, allowing for subsequent reversal to a sol state. Our scheme for photogelation of alginate

is illustrated in Figure 3.1. The components of the aqueous system are sodium alginate, an insoluble calcium salt, typically calcium carbonate ($CaCO_3$), and the photoactive PAG component, which here is diphenyl-iodinium nitrate. When the sample is irradiated with UV light, the PAG gets photolyzed to generate acid (H^+). The acid triggers the dissolution of $CaCO_3$ to generate free Ca^{2+} ions by the reaction shown. The Ca^{2+} ions then electrostatically bind to the L-guluronate (G) blocks of adjacent alginate chains to create crosslinks ("egg-box" junctions),[18,47] and in the process an alginate gel is formed. The same method can be used with other Ca^{2+}-responsive biopolymers, and we demonstrate this with a second polysaccharide, pectin. The gels are also shown to be reversible by addition of calcium chelators like sodium citrate. We note that our approach is analogous to gelation of alginate by *in situ* dissolution of an insoluble calcium salt upon the slow hydrolysis of D-glucono-δ-lactone (GdL) to gluconic acid – the difference here is that acid formation is triggered by light via the PAG.[7,48]

Photogellable alginate solutions may be useful for the encapsulation of cells or biomolecules, especially since the use of light allows gelation to be realized in a local and spatially selective manner. Recently, there has been considerable interest in producing micro- or meso-scale patterns of alginate gels or films on various substrates as a means to interface soft biological components to hard devices.[10,49,50] Towards this end, we demonstrate herein the creation of microscale, chemically erasable patterns of alginate hydrogel films using our photogellable alginate in conjunction with rudimentary photolithographic techniques

3.2. EXPERIMENTAL SECTION

Materials. Sodium alginate (product number W201502) was purchased from Sigma-Aldrich. Its molecular weight was specified to be in the range of 12–40 kDa. Low-methoxy (LM), deamidated pectin from fruit (product number 400505) was purchased from Carbomer. Its molecular weight was specified to be 500–600 kDa while its degree of esterification was 33–35%. Precipitated calcium carbonate ($CaCO_3$) particles (mean particle radius of 70 nm) were obtained from Specialty Minerals, Birmingham, UK. Diphenyliodonium nitrate, a type of photoacid generator (henceforth abbreviated as PAG), was purchased from Sigma-Aldrich. Quantofix® calcium indicator strips were purchased from CTL Scientific. The calcium chelator salt, sodium citrate dihydrate (NaCit) was purchased from Fisher Scientific. Distilled-deionized (DI) water was used for all the experiments.

Sample Preparation. Samples were prepared by combining the $CaCO_3$ particles with a solution of sodium alginate and PAG in DI water. Each mixture was stirred overnight by a magnetic stirrer bar and was then sonicated using a Branson 1510 sonicator for 45 min at 40 kHz. Stock samples of 10-15 mL were prepared to enable multiple experiments. A similar procedure was used with the pectin samples; However, because the as-supplied pectin gave an acidic solution, it was first neutralized with 0.01 M NaOH to a pH 7 before adding the PAG and $CaCO_3$.

Sample Response Before and After UV Irradiation. Samples were irradiated with UV light from an Oriel 200 W mercury lamp. A dichroic beam turner with a mirror

reflectance range of 280-400 nm was used along with a filter (< 400 nm) to access the UV range of the emitted light. Samples (2 mL) were placed in either a Petri dish of 60 mm diameter or a 20 mL vial, covered with a quartz cover glass, and irradiated by UV through the cover. During irradiation, the sample was stirred by a magnetic stirrer bar.

Rheological Studies. An AR2000 stress-controlled rheometer (TA instruments) was used to perform steady and dynamic rheology experiments. All rheological experiments were done at 25°C using a cone-and-plate geometry (40 mm diameter and 2° cone angle). A solvent trap was used to minimize drying of the sample during measurement. Dynamic stress sweep experiments were first performed on a sample to identify its linear viscoelastic (LVE) region and dynamic frequency sweeps were then performed within the LVE region.

Hydrogel Patterning. 500 μL of a given sample was smeared on a portion of a glass slide and this region was then exposed to UV through a homemade photomask or stencil. After 20-25 min of UV exposure, the slide was rinsed with 1% NaCl to wash off the ungelled portions, thus revealing the photopatterned features. Certain samples were doped with a small amount of fluorescently-labeled, carboxylate-modified polystyrene latex particles (2 μm diameter; from Sigma-Aldrich), and the corresponding patterns were imaged by a fluorescence microscope (Olympus MVX10 Macroview). Images were analyzed using ImageJ software from NIH to quantify fluorescence intensity.

3.3. RESULTS AND DISCUSSION

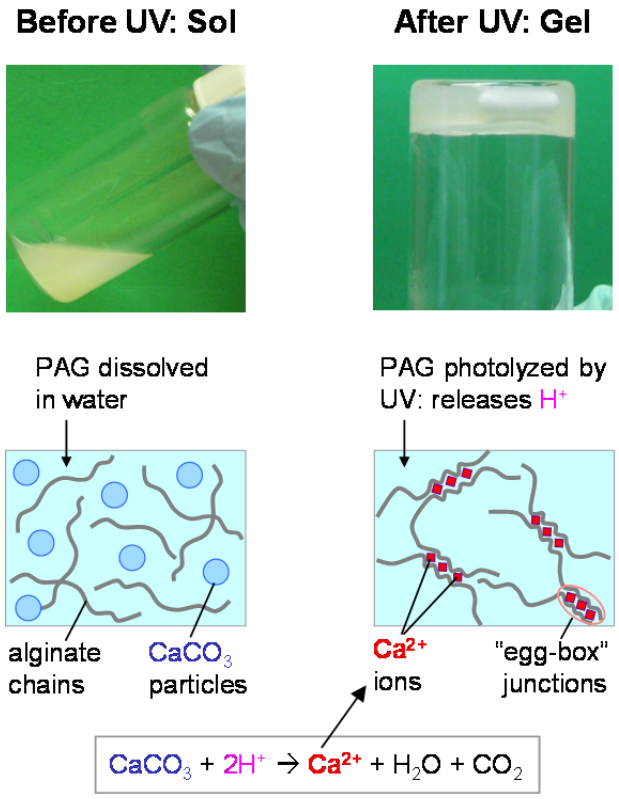

Figure 3.1. Schematic and visual depiction of UV-induced alginate photogelation. Sodium alginate (2 wt%) is combined with 15 mM of $CaCO_3$ particles (insoluble) and 30 mM of a photoacid generator (PAG). The resulting sample is a turbid dispersion (sol) and flows freely in the vial. Upon exposure to UV light, the PAG gets photolyzed and thereby releases H^+ ions, which react with the $CaCO_3$ to form soluble Ca^{2+} ions. These ions gel the alginate, and the sample holds its weight upon vial inversion. The crosslinks in the gel are domains of Ca^{2+} bridging adjacent chains, as shown in the schematic, and these are referred to as "egg-box" junctions

Figure 3.1 visually demonstrates the photogelling response of an alginate sample. The Ca^{2+}-induced gelling ability of alginate is known to depend on its ratio of α-L-guluronate (G) to β-D-mannuronate (M) units. It is the G units that have the ability to bind to Ca^{2+} ions, and for inter-chain crosslinking to occur, blocks of G units on adjacent chains must come into close proximity (resulting in "egg-box junctions"),[18,47] as depicted

in Figure 3.1. For our photogelling experiments, we typically prepared a sample of 2 wt% of sodium alginate, 30 mM of solubilized PAG, and 15 mM of dispersed $CaCO_3$ particles. The particles were a nanosized precipitated form of $CaCO_3$, with a mean particle radius of ~ 70 nm as stated by the manufacturer and confirmed by us using dynamic light scattering (DLS). Using sonication, these particles could be homogeneously dispersed in the polymer solution. No aggregation or settling of the particles was observed over a period of several hours after sonication, during which time the UV irradiation was conducted. As shown by the photograph in Figure 3.1, the initial mixture is a low-viscosity sol. When exposed to UV light for 45 min, the PAG gets photolyzed, releasing acid (H^+).[42-45] The acid reacts with the insoluble $CaCO_3$ particles to generate free Ca^{2+} ions, which crosslink the alginate chains into a gel network.[7,48] The resulting alginate gel is strong enough to hold its weight in the inverted vial (Figure 3.1); note also the stirrer bar trapped in the gel.[51]

The above rheological changes were quantified using dynamic rheology. Frequency spectra, i.e., plots of the elastic modulus G' and the viscous modulus G'' as functions of the frequency ω, are shown in Figure 3.2A for the above sample before and after UV irradiation. Before UV irradiation, the alginate/$CaCO_3$/PAG mixture responds as a purely viscous sol: i.e., its G'' is a strong function of ω ($G'' \sim \omega^1$) while its G' is too small to be measured accurately.[52] On the other hand, after 45 min of UV exposure, the sample shows an elastic, gel-like response: i.e., in this case, G' exceeds G'' over the range of frequencies tested and also G' is nearly independent of frequency.[52] From the data, the gel modulus (i.e., the value of G' as $\omega \to 0$) is about 40 Pa, which is comparable to

moduli reported previously for Ca^{2+}-induced gels of alginate at similar concentrations.[7] Note that the value of the gel modulus depends on the source of the alginate, which influences its molecular weight, its ratio of G to M units, and the blockiness (distribution pattern) of the G units.[7,17]

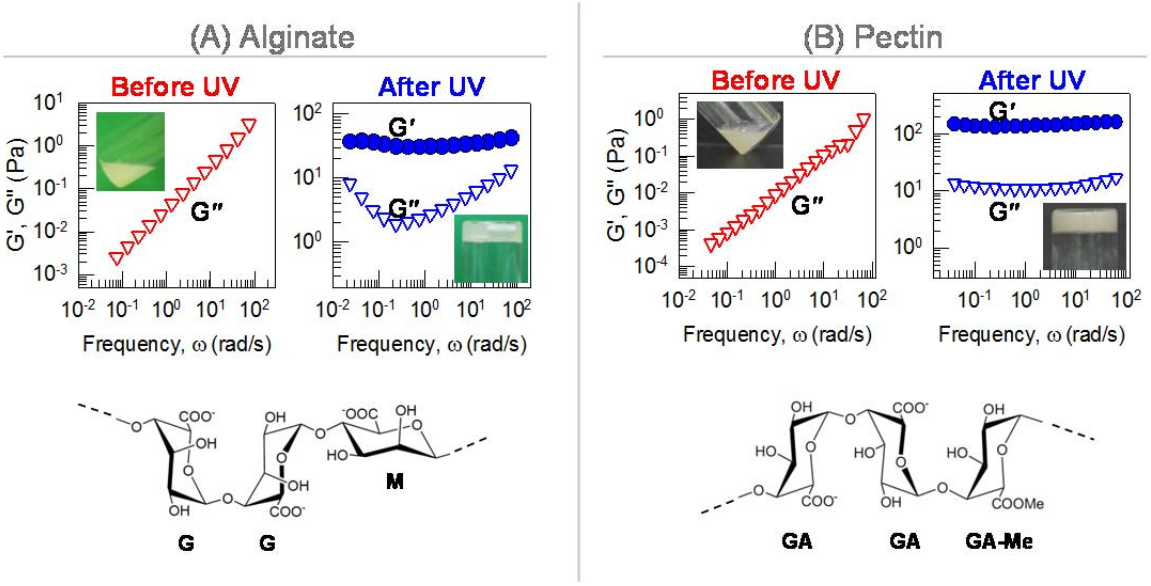

Figure 3.2: Dynamic rheological data demonstrating photogelling of aqueous solutions of two biopolymers: (A) alginate (2 wt%) and (B) pectin (0.9 wt%). In each case, the sample also contains 15 mM of $CaCO_3$ and 30 mM of PAG. Before UV irradiation, both samples show a viscous response, with the viscous modulus G'' varying strongly with frequency and the elastic modulus G' being negligible. After 45 min of UV irradiation, the samples are both converted into gels, which show an elastic response, i.e., $G' > G''$ and with the moduli being nearly independent of frequency. The chemical structures of the two polymers are also shown.

To confirm the generality of our approach, we investigated photogelation of another biopolymer, pectin, which is also known to undergo Ca^{2+}-induced crosslinking.[17,46] Pectin is a polymer composed mostly of α-D-galacturonate (GA) residues, and its structure is shown in Figure 3.2B. In the case of a low-methoxy (LM) pectin, such as the one used here, a fraction of the carboxylic acid groups are esterified with methanol. Short blocks of GA units from adjacent chains can interact with Ca^{2+} ions, resulting in "egg-box junctions" (much like in the case of alginate; note that GA and G are almost mirror images) and thereby a hydrogel. [17,46] We used a 0.9 wt% solution of LM pectin, which was first neutralized with NaOH to a pH of 7 and then combined with 30 mM of PAG and 15 mM of $CaCO_3$ particles. The above mixture is initially a low-viscosity sol, as indicated by its dynamic rheological response in Figure 3.2B: i.e., here again, its $G'' \sim \omega^1$ while its G' is too low to be measured accurately. Upon UV irradiation for 45 min, the sample is transformed into a gel that holds its weight upon vial inversion. Dynamic rheology confirms the gel-like character: i.e., G' exceeds G'' over the range of frequencies and both moduli are nearly independent of frequency. Note that the gel modulus in the case of 0.9% pectin is about 150 Pa, which is higher than that of the 2% alginate gel.

The above results show that our photogelation scheme can be easily applied to any Ca^{2+}-responsive polymer without the need for any prior synthesis step. As stated earlier, the mechanism for photogelation involves release of free Ca^{2+} upon reaction with H^+ produced by PAG photolysis. This mechanism is supported by a series of control experiments and related observations. As a first control, we confirmed that mixtures of

sodium alginate with $CaCO_3$ (i.e., in the absence of PAG) did not gel upon exposure to UV radiation. Similarly, mixtures of alginate and PAG (i.e., in the absence of $CaCO_3$) also showed no gelation upon exposure to UV light. Next, we measured pH changes caused by UV irradiation in samples containing alginate/PAG and alginate/PAG/$CaCO_3$. In the former case, the pH dropped from ~ 7 to ~ 4, while in the latter case, the pH drop was from ~ 9 to ~ 7.4. These pH changes are consistent with release of acid upon PAG photolysis; the reason why the pH changes are not identical for the two cases is probably due to the buffering ability of Ca^{2+} salts. Next, we used a Ca^{2+} indicator strip to qualitatively confirm the UV-induced release of free Ca^{2+} when PAG and $CaCO_3$ are both present. Together these results indicate that: (a) both PAG and $CaCO_3$ are required for photogelation; (b) photolysis of PAG releases H^+; and (c) the reaction of H^+ and $CaCO_3$ generates free Ca^{2+}, which as expected, is effective at crosslinking alginate.

To further probe the photogelation phenomenon, we performed additional experiments with alginate. First, the effect of UV irradiation time was studied and the results are shown in Figure 3.3. The sample again consisted of 2% alginate, 30 mM PAG and 15 mM $CaCO_3$. 2 mL of the above sample was irradiated for different lengths of time, followed by rheological testing. Data from steady-shear rheology for the apparent viscosity vs. shear stress are shown in the figure. We plot the data vs. shear stress (rather than shear rate) because it clearly reveals the emergence of a yield stress in the sample. Before UV irradiation, the sample is a Newtonian liquid with a viscosity of 28 mPa.s. No appreciable changes in rheology occur with 5 min of UV exposure. However, after 10 min of UV exposure, the sample viscosity is enhanced by a factor of 10^5 at low shear

stresses followed by a shear-thinning response at higher shear stresses. Further exposure to UV causes continued growth in the low-shear viscosity. After 45 min of UV exposure, the viscosity is very high (essentially infinite) at low shear stresses and then drops sharply around a stress of 3 Pa (which then is the yield stress of this sample[52]). Further UV exposure up to 120 min causes the yield stress to increase to ~ 8 Pa. Taken together, the data show that a macroscopic sample (2 mL) requires tens of minutes to reach a photogelled state. However, the rate of photogelling appears to be controlled by the rate of UV absorption by the PAG molecules (once UV is absorbed, the PAG photolyzes in nanoseconds).[37,40] This means that more rapid photogelling can be achieved for small sample volumes, and indeed this will be seen later in our experiments with thin alginate films. Similar trends in kinetics have been noted for other self-assembly-based photorheological fluids.[37,40]

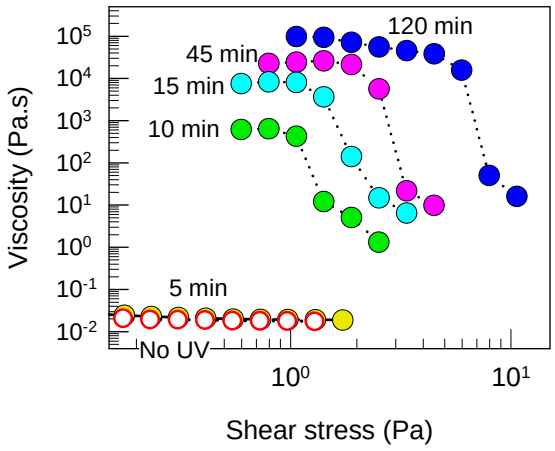

Figure 3.3. Effect of UV irradiation time on sample rheology. Steady-shear rheological data are shown for a sample containing 2% Alginate + 15 mM $CaCO_3$+ 30 mM PAG before and after UV irradiation for various periods of time. The sample is transformed from a low-viscosity, Newtonian fluid to a gel with a yield stress

Next, we studied the effect of PAG concentration on photogelling. For this, we fixed a mixture of 2% alginate and 15 mM $CaCO_3$, and to this we added varying amounts of PAG (5 to 30 mM). Steady-shear rheological data for the viscosity vs. shear stress are shown in Figure 3.4 for these samples after 45 min of UV exposure. The initial (before UV) viscosities of the samples were low and identical (data not shown). Samples with low amounts of PAG (5 or 10 mM) did not show a change in viscosity upon UV irradiation. However, samples with higher concentrations of PAG (13 or 30 mM) underwent photogelling, i.e., a significant (> 10^5) increase in low-shear viscosity and the emergence of a yield stress can be seen in Figure 3.4 for these samples. Thus, a minimum amount of PAG (> 13 mM) is required for photogelling a given alginate/$CaCO_3$ sample. The above amount presumably correlates with the minimum concentration of Ca^{2+} required to form a sample-spanning network of alginate chains.

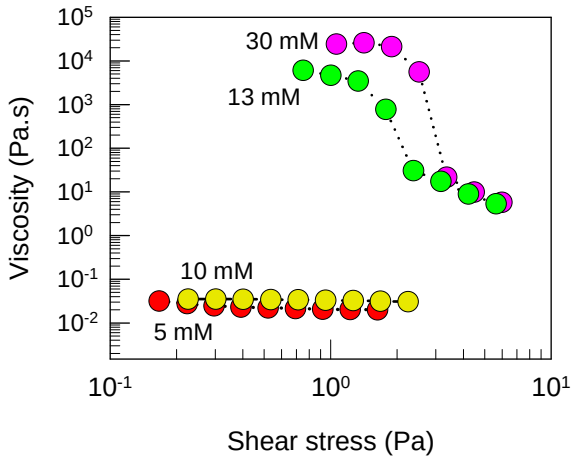

Figure 3.4. Effect of PAG concentration on photogelling. Steady-shear rheological data are shown after 45 min of UV irradiation for samples containing 2% Alginate + 15 mM $CaCO_3$ + varying amounts of PAG.

We then studied the effect of alginate concentration on photogelling. In this case, samples with 15 mM $CaCO_3$ and 30 mM PAG were combined with varying amounts of alginate (0.5 to 3.5 wt%). The samples were UV-irradiated for 45 min and then studied by dynamic rheology (Figure 3.5). All samples exhibited a viscous response before UV irradiation (data not shown). After UV irradiation, the sample containing 0.5% alginate shows a viscous or viscoelastic response in a dynamic frequency sweep (i.e., $G'' > G'$, with both moduli varying strongly with frequency). Presumably, there are not enough alginate chains to form a sample-spanning network at this concentration. In comparison, samples with higher concentrations of alginate (1, 2, and 3.5%) all show a gel-like frequency response after UV exposure (i.e., $G' > G''$ and negligible frequency dependence of the moduli). The alginate concentration only has a modest effect on the gel modulus, however: e.g., the modulus of the 3.5% alginate sample is only a factor of 2 higher than that of the 1% alginate sample.

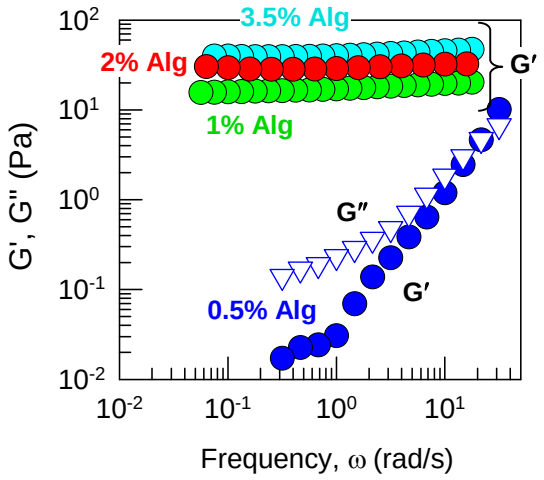

Figure 3.5. Effect of alginate concentration on photogelling. Dynamic rheological data are displayed after 45 min of UV irradiation for samples containing different concentrations (wt.%) of sodium alginate along with 15 mM of $CaCO_3$ and 30 mM of PAG. For the 0.5% alginate sample, both G' and G'' are shown while for the rest of the samples, only G' is shown.

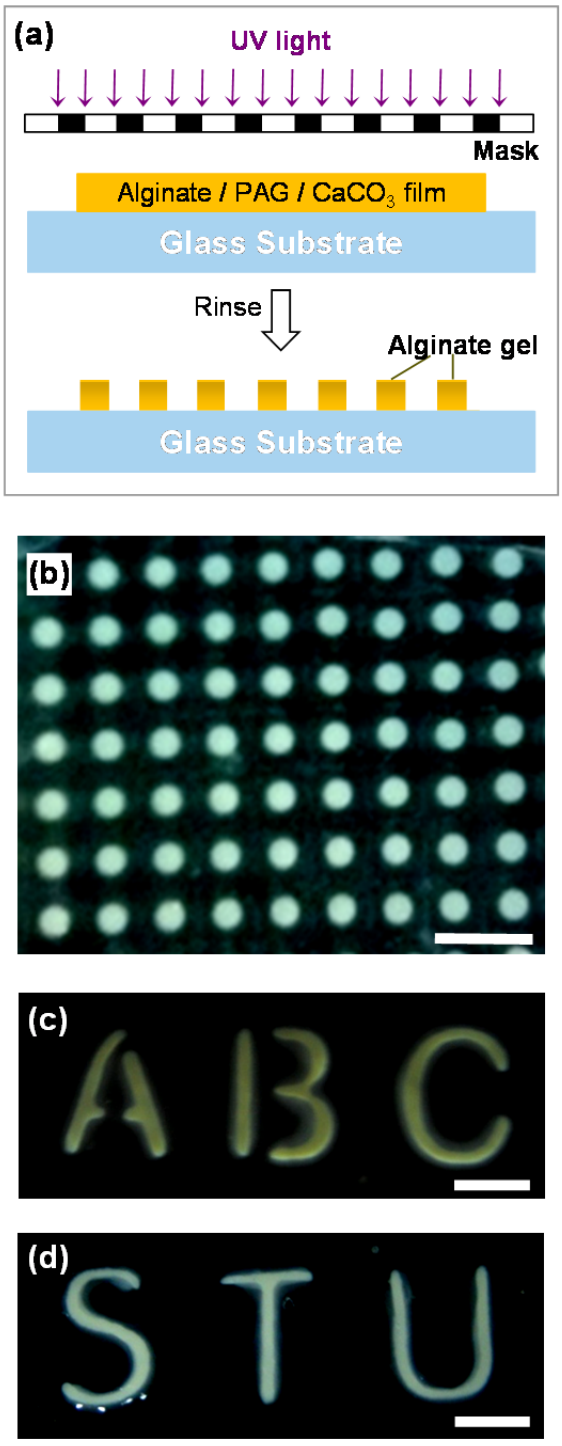

Figure 3.6. (a) Schematic depiction of alginate photopatterning. The photogellable alginate sample is spread as a thin film and UV-irradiated through a mask. After rinsing, gelled regions corresponding to the pattern in the mask are revealed. (b) Alginate gel patterned as an array of ~ 900 mm dots using a steel photomask. Scale bar is 3 mm. (c), (d) Alginate gel patterned as adjacent letters of the alphabet using a stencil. Scale bars represent 5 mm.

The above photogels of alginate and pectin can be easily converted back to solution state by addition of a calcium chelator such as sodium citrate (NaCit). Such chemical reversibility can be a useful property because it can allow entrapped species within a gel to be subsequently released. Here, we studied chemical reversibility of alginate photogels using NaCit. We began with a sample of 2% alginate, 30 mM PAG and 15 mM $CaCO_3$, which was then exposed to UV to 45 min to create a photogel. To this we added a small amount (2 μL) of concentrated NaCit solution so as to bring the overall NaCit concentration in the sample to 100 mM. As expected, the sample immediately ungelled into a freely flowing solution because the Ca^{2+} cations detached from the alginate chains and instead became preferentially bound to the citrate anions.

Finally, we describe the use of our photogellable alginate formulation for creating patterned films of alginate gels. As mentioned in the Introduction, there is considerable interest from the biomaterials community in forming patterns of alginate gels on various substrates.[10,49,50] Such patterns have been created thus far mostly using chemical[49,50] or electrochemical[10] techniques. If patterning could instead be done by light,[9] it would be easier, more convenient, and potentially amenable to higher resolutions. Moreover, photopatterning could make use of the techniques and infrastructure currently employed in photolithography. Here, as an initial step in this direction, we demonstrate a few basic photopatterning experiments with alginate. The inherent idea, as shown by Figure 3.6a, is that when a thin layer of alginate/$CaCO_3$/PAG is exposed to UV light through a patterned mask, only the exposed regions get crosslinked into a solid gel. The unexposed areas can then be washed away to reveal the pattern corresponding to the mask. Figure 3.6b-d show

a few simple patterns created using a steel photomask with equally spaced holes or a commercial stencil. In this case, we used a mixture of 3 wt% alginate, 15 mM of $CaCO_3$, and 70 mM of PAG as the sample formulation. This liquid sample was spread as a thin layer on a glass slide and UV-irradiated through the mask/stencil for 20-25 min, followed by rinsing with 1% NaCl. As can be seen, alginate gel films are formed on the glass slide in patterns corresponding to the respective masks, i.e., an array of microdots in the case of the steel mask (Figure 3.6b) and letters from the alphabet in the case of the stencil (Figure 3.6c,d).

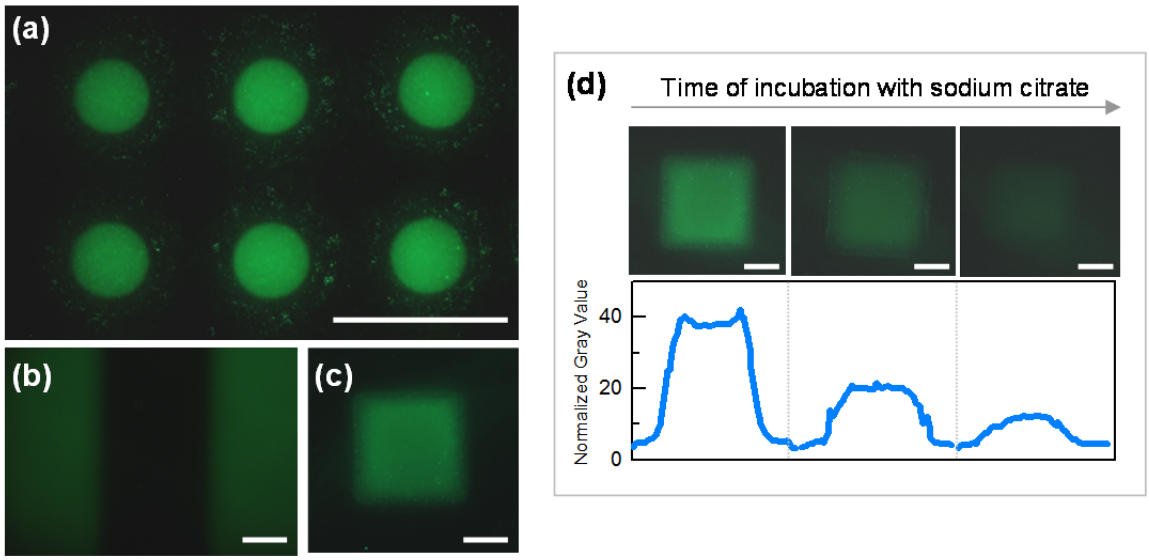

Figure 3.7. (a), (b), (c) Patterns of alginate gel with embedded fluorescent microparticles. Three different patterns are shown: (a) dots; (b) stripes; (c) squares, and in each case, the patterned regions shows green fluorescence from the microparticles. (d) Pattern erasure by incubation with sodium citrate (NaCit). The fluorescence intensity is observed to decrease with incubation time, and this is quantified in the plot. Scale bars in all images correspond to 2 mm.

Next, we show the use of these patterned gels for entrapment and release of microstructures. We used fluorescently labeled polystyrene latex microparticles (2 μm diameter) as a model payload, and we added these particles to the above sample of alginate/PAG/$CaCO_3$. The resulting mixture was used to pattern gels of alginate on a glass slide using either the steel mask from above or other homemade masks. Images of the patterns via a fluorescence microscope are shown in Figure 3.7 and all the patterns are observed to show green fluorescence due to the embedded microparticles. We then took the square pattern and exposed it to 10 mM of NaCit solution. As shown by the time-lapse images in Figure 3.7d, the fluorescence from the patterned region decreased with time, and this decrease is quantified by the plots in Figure 3.7d. This pattern was completely erased in 50 mins under mild stirring. The decrease in fluorescence is due to the NaCit-induced erosion of the alginate matrix and the resultant release of the entrapped microparticles. Thus, patterns of alginate can be chemically erased under mild conditions, allowing release of embedded microstructures. The results suggest that our photogellable alginate formulation could be a useful material for interfacing cells or biomolecules to substrates in a spatially controlled fashion.

3.4. CONCLUSIONS

We have presented a simple photogelation scheme for alginate and other biopolymers, wherein we combine alginate with nanoparticles of insoluble $CaCO_3$ and a PAG. Upon exposure to UV, the PAG generates H^+ ions, which solubilize the $CaCO_3$ to produce free Ca^{2+}, and these ions in turn crosslink the alginate into a gel. The scheme was extended to pectin in this study, and it can also be applied to other Ca^{2+}-sensitive biopolymers. The method is simple because it involves no chemical modification of the parent polymers and uses relatively inexpensive, commercially available components. We have also used our photogellable alginate in photopatterning studies, wherein a patterned alginate gel is formed on a glass substrate by irradiating the solution through a photomask. The patterned gels can be used to immobilize payloads such as microparticles, and the patterns can be subsequently erased under mild conditions by subjecting the gels to a calcium chelator. We expect that photogellable alginate will prove to be a useful material for building the biology-device interface.

Chapter 4

ENZYMATIC GELATION OF ALGINATE

The results presented in this chapter have been published in the following journal article: Yi Liu,* Vishal Javvaji,* Srinivasa R. Raghavan, William E. Bentley and Gregory F. Payne, "Glucose Oxidase-Mediated Gelation: A Simple Test to Detect Glucose in Food Products." *Journal of Agricultural and Food Chemistry*, 60, 8963−8967 (2012).

* These authors made equal contributions.

Author Contributions:

The concept of enzymatic gelation of alginate was conceived by VJ and GFP. The use of this gelation for detecting sugars was conceived by GFP and YL. Implementation of these concept was spearheaded by YL and VJ. Rheological experiments and analysis were performed by VJ while the sugar detection experiments were performed by YL. YL wrote the first draft of the manuscript with input from VJ, which was then edited and critically reviewed by all the authors.

4.1. INTRODUCTION

Economic, political, and climatic instabilities affect the global sugar market, and historically the U.S. price for table sugar (sucrose) has been substantially higher than world prices. The abundance of starch and thus glucose syrup was an attractive alternative, but glucose is less sweet than sucrose. The discovery that the enzyme xylose isomerase could catalyze the conversion of glucose to the sweeter monosaccharide fructose[54] coupled with advances in enzyme immobilization enabled the creation of large-volume processes to generate high-fructose corn syrup (HFCS).[55] HFCS emerged as a less expensive sweetener (compared to sucrose) and was broadly accepted into the marketplace (e.g., soft drinks) beginning in the early 1970s.[56-58] At the same time that HFCS emerged as a major sweetener, there was an increase in the incidences of obesity and diabetes in affluent countries (e.g., the United States) leading to hypotheses and controversies over whether the timing of these observations reflects a coincidental correlation or a causal relationship.[58-61]

Whereas the relative merits of sugar, glucose, and HFCS may be unresolved scientifically,[62] many consumers have formed preferences and purchase products on the basis of the labeled ingredient statements.[63] Unfortunately, ingredient statements may not be entirely trustworthy when a product is manufactured from many ingredients, each of which may have a supply chain that spans continents, cultures, and languages. Furthermore, strong cost incentives may encourage adulteration by substituting lower cost sweeteners (e.g., HFCS) for more expensive sugar. The existence of glucose in HFCS and other artificial sweeteners makes it a potential marker for the detection of non-

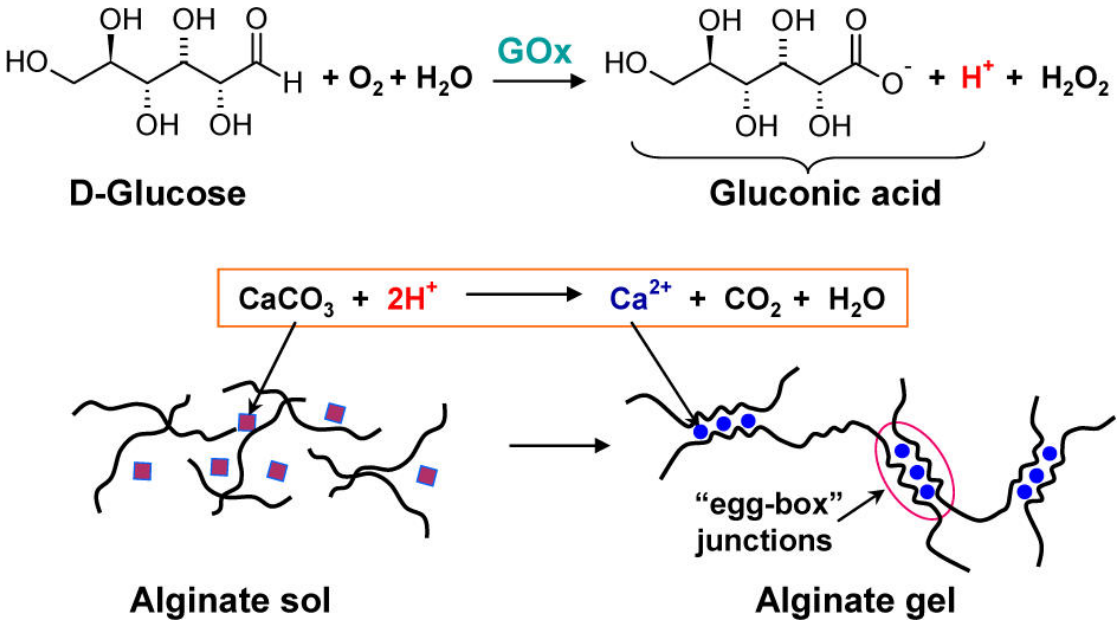

Figure 4.1 Schematic illustration of glucose oxidase (GOx)-mediated gelation of alginate. GOx-catalyzed oxidation of glucose generates protons, which solubilize the Ca^{2+} ions that trigger alginate's hydrogel

sucrose sweeteners. Thus, a simple method to detect glucose on-site or in the home may allow buyers or consumers to make more informed decisions. Analysis of glucose in foods and beverages is challenging because of the complexity of the matrix and the structural similarities of various components (e.g., other sugars). A similar challenge was faced in the development of in-home tests for blood glucose, which became integral to the individualized management of diabetes.[64-67] In this case, enzymes such as glucose oxidase (GOx) were enlisted to "recognize" glucose and generate an electrochemically active species (e.g., H_2O_2) that allows transduction into an electrical output.[68-70] Here, we also enlist glucose oxidase to recognize glucose, but we transduce this recognition into a visually observable mechanical output.

Figure 4.1 schematically illustrates the recognition−trans-duction approach used to detect glucose by inducing gelation of the polysaccharide alginate. First, GOx

catalyzes the oxidation of glucose in the presence of oxygen to generate gluconic acid and hydrogen peroxide.[71-73] The in situ-generated gluconic acid dissociates, and the protons react to solubilize $CaCO_3$ and release Ca^{2+} ions. The released Ca^{2+} interacts with alginate to form the "egg-box" network junctions that serve as the physical cross-links responsible for the gelation of calcium alginate hydrogels.[10,74-78]

Here, we demonstrate that the GOx-mediated oxidation of glucose can trigger gelation of the common food biopolymer alginate. GOx confers sugar selectivity to this process, whereas gel formation is a readily observable measure that requires no specialized instrumentation and is insensitive to color in the sample (compared to color-based tests).

4.2. EXPERIMENTAL SECTION

Materials. The following materials were purchased from Sigma-Aldrich: alginic acid sodium salt from brown algae (medium viscosity, molecular weight 80−120 kDa), D-(+)-glucose (≥99.5%), D-(−)-fructose (≥99%), sucrose (≥99.5%), and GOx from Aspergillus niger (138800 U/g). Precipitated calcium carbonate ($CaCO_3$) particles (70 ± 21 nm as reported by the manufacturer) were obtained from Specialty Minerals, Birmingham, UK. Syrup, table sugars, and beverages were purchased from local grocery stores.

Sample Preparation. Alginate solutions (1−1.5%) were prepared by dissolving sodium alginate powder in distilled water, followed by stirring overnight; then $CaCO_3$ (20−30 mM) particles was dispersed into sodium alginate solution, followed by ultrasonication for 30 min. These alginate and $CaCO_3$ levels are in excess of those required to form strong self-supporting gels. The alginate/$CaCO_3$ thus prepared (pH ∼8.0) was stirred before use to ensure the particles remained homogeneously dispersed in the alginate solution. No aggregation or settling of the particles was observed over a period of several hours, during which time the gel-forming experiments were conducted. GOx solution was prepared by dissolving GOx (1000 U/mL) in phosphate-buffered saline (20 mM, pH 7.4). Purified sugars (glucose, fructose, or sucrose) were dissolved in water to a concentration of 0.5 M before use. Food products (e.g., beverages) containing different sugar-based sweeteners were diluted in water to levels of 30 mg sugars/mL on the basis of information provided on the ingredient statement.

Gel Formation. Typically, we prepared a stock suspension containing GOx (10 U/mL)/alginate (1.5%)/$CaCO_3$ (30 mM) and then mixed this stock suspension with a diluted solution containing the sugar-based product (30 mg sugars/mL). The mixed suspension (pH ~7.5) was briefly vortexed and exposed to air for 1−3 h. Photographs were typically taken 1 h after the mixing**.**

Rheology. Rheological measurements were performed on a Rheometrics AR2000 stress-controlled rheometer (TA Instruments). A cone-and-plate geometry of 40 mm diameter with a 2° cone angle was used with a solvent trap to prevent drying. Time sweeps were typically performed at 10 rad/s with strains of 25−30% for liquid-like samples and 1% for gel-like samples. Dynamic stress sweep experiments were first performed on a sample to identify its linear viscoelastic (LVE) region, and dynamic frequency sweeps were then performed within the LVE region. All rheological experiments were conducted at 25 °C.

4.3. RESULTS AND DISCUSSION

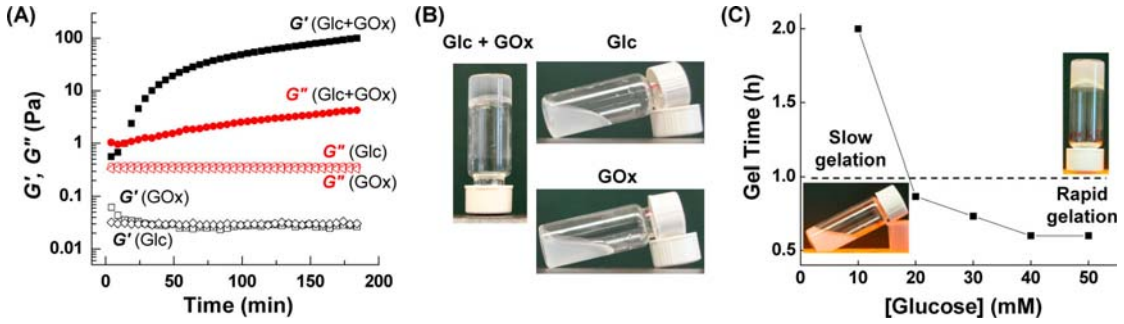

Figure 4.2. Demonstration that the GOx-catalyzed oxidation of glucose (Glc) triggers alginate gelation. (A) Time sweeps of rheological measurements show that both GOx (10 U/mL) and Glc (40 mM) are required to induce gelation of a mixture of alginate (1%) and $CaCO_3$ (20 mM). (B) Vial inversion tests provide visual evidence that both GOx and Glc are required to form a self-supporting gel in 1 h. (C) Vial inversion tests show that gels

In our initial study, we used rheology to demonstrate GOx-mediated gelation of an alginate/$CaCO_3$ suspension. In the first experiment, a mixture of alginate (1%), $CaCO_3$ (20 mM), and glucose (40 mM) was prepared, and GOx (10 U/mL) was added to initiate the reaction. This sample was loaded onto the rheometer stage that had been set to 25 °C, and data were recorded 4 min after initiation of the reaction. Figure 4.2A shows that when GOx was added to the glucose/alginate/$CaCO_3$ suspension, the elastic modulus (G′) and viscous modulus (G″) increased during the 180 min experiment. The increase in G′ was faster than that in G″, and after 14 min G′ exceeded G″, indicating that the solution was transitioning into a gel.[79] Figure 4.2A also shows results for two controls lacking either glucose or GOx. For both controls, the moduli remained small and nearly constant over the course of the experiment, and G″ exceeded G′. These observations indicate that

the controls remained solutions throughout the 180 min experiment. Thus, the results in Figure 4.2 provide a rheological demonstration that the GOx¬mediated oxidation of glucose can trigger the gelation of alginate as proposed in Figure 4.1

Gel formation is a simple end-point measurement as it can be detected visually without the need for instrumentation.[51] For instance, the results in Figure 4.2A can be reproduced qualitatively using a vial inversion test. For this test, we mixed alginate (1%), $CaCO_3$ (20 mM), GOx (10 U/mL), and glucose (40 mM) in a 4 mL vial and exposed this mixture to air. Figure 4.2B shows that after 1 h of incubation, the vial could be inverted and the hydrogel that had formed could support its own weight. Controls lacking either Glc or GOx did not form gels as evidenced by the fact that they remained liquids as shown in Figure 4.2B

The limit for detecting glucose by a vial inversion method was estimated by observing gel formation at various glucose concentrations. In this experiment, we mixed alginate (1%), $CaCO_3$ (20 mM), and GOx (10 U/mL) with various amounts of glucose and periodically observed whether the vial's contents had undergone gel formation. Figure 4.2C shows that the gel time (the time required to form a self-supporting gel) decreased with increasing glucose concentration. Solutions prepared with >20 mM glucose formed gels within 1 h, whereas solutions prepared with 10 mM glucose formed weak gels only after 2 h of incubation. Solutions prepared with 5 mM glucose did not form gels even after overnight incubation. The photographs inserted in Figure 4.2C show

the vials for 10 and 50 mM samples after being incubated for 1 h. If we use 1 h as a reasonable incubation period, Figure 4.2C indicates that 20 mM is the limit for glucose detection by this vial inversion method. This detection limit is an order-of-magnitude lower than glucose levels typically present in beverages sweetened with HFCS. [80]

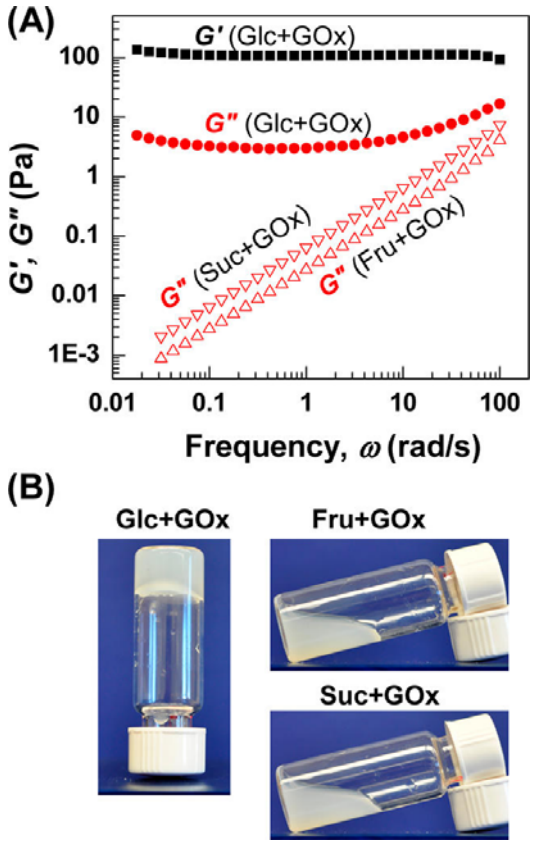

Figure 4.3. GOx confers sugar selectivity to alginate gelation. (A) Dynamic frequency sweeps demonstrate that a suspension of GOx (10U/mL)/alginate (1%)/$CaCO_3$ (20 mM) forms a hydrogel in the presence of 40 mM glucose (Glc) but not fructose (Fru) or sucrose (Suc) (samples incubated in air for 3 h; G′ values for controls were too low to measure accurately). (B) Vial inversion tests demonstrate sugar selectivity of GOx-mediated gel formation.

Next we examined the sugar specificity of the GOx-mediated gel formation. In this study, 40 mM glucose, fructose, or sucrose was added into a suspension of alginate (1%), $CaCO_3$ (20 mM), and GOx (10 U/mL), and these mixtures were exposed to air for

3 h. After incubation, the samples were loaded onto the rheometer stage and dynamic frequency sweeps were performed. Figure 4.3A shows that when glucose was present, the sample behaved as a soft solid with G′ exceeding G″ and both moduli being nearly independent of frequency. This behavior is consistent with the formation of a gel from the glucose-containing solution. Figure 4.3A also shows that the sucrose and fructose controls behave as viscous liquids with the viscous modulus (G″) varying strongly with frequency (note: the elastic modulus G′ is not shown for these controls because it was too low to be measured accurately). The rheological behavior for these controls confirms that neither fructose nor sucrose can induce a gel formation in the presence of glucose.

The sugar selectivity for GOx-mediated alginate gelation is also apparent using a vial inversion approach. Using the same experimental conditions as for the above rheology experiment, Figure 4.3B shows that glucose (but not fructose or sucrose) triggers gel formation for the GOx/alginate/$CaCO_3$ mixture. Thus, Figure 4.3 demonstrates that GOx confers sugar selectivity to gel formation, and this gel formation can be observed without the need for complex instrumentation.

In subsequent studies, we examined the ability of this GOx-mediated gelation method to detect glucose in food products. For this, we prepared a stock suspension containing GOx (10 U/mL)/alginate (1.5%)/$CaCO_3$ (30 mM). Two parts of this stock suspension were mixed with 1 part of a sugar-containing product that had been appropriately diluted (30 mg sugars/ mL) to obtain a reaction suspension containing 10 mg/mL sugar.

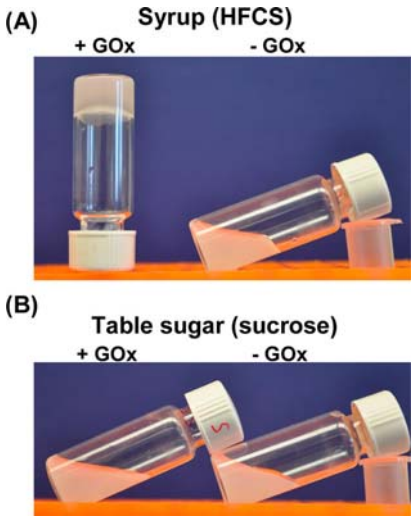

Figure 4.4 GOx-mediated gel formation for samples containing highfructose corn syrup (HFCS) but not table sugar (sucrose). (A) Vial inversion tests show that HFCS induces gelation, whereas results from the control lacking GOx indicate that other ingredients in the syrup do not induce gelation. (B) Vial inversion tests show that table sugar does not induce gel formation. Samples were prepared by mixing 1 part of a solution containing sugar product (30 mg sugars/mL) with 2 parts of a stock suspension containing GOx (10 U/mL)/alginate (1.5%)/$CaCO_3$ (30 mM).

Our first sample was store-bought syrup containing HFCS. After mixing the diluted syrup with the stock suspension, the vial was left in air over 1 h. As shown in Figure 4.4A, a self-supporting gel was formed, indicating the presence of glucose (from HFCS). Concurrently, a control mixture lacking GOx was prepared, and Figure 4.4A shows that no gel formation was observed. Results from this control indicate that other ingredients in the syrup do not induce gel formation

Next we tested table sugar (pure cane sugar) by mixing a solution of this sugar with the stock suspension and exposing the sample to air for 1 h. As expected, Figure 4.4B shows gels were not formed for samples containing table sugar either with or without GOx. Thus, Figure 4.4 shows that GOx-mediated alginate gelation can detect glucose in the syrup and distinguish it from table sugar

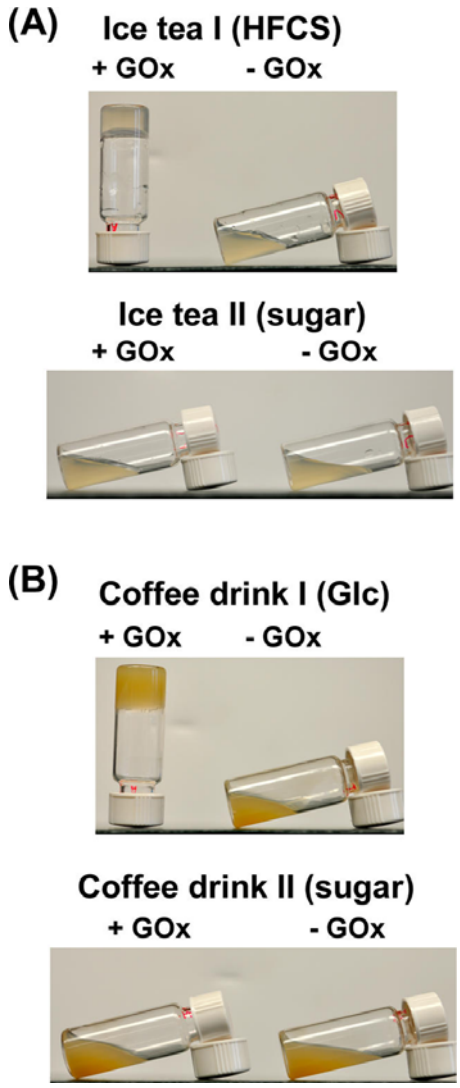

Figure 4.5. GOx-mediated gel formation to "detect" non-table sugar sweeteners in selected beverages. (A) Vial inversion tests show gelation with an ice tea containing HFCS (ice tea I), but not with an ice tea containing "sugar" (ice tea II). (B) Vial inversion tests show gelation with a coffee drink containing glucose (coffee drink I) but not with a coffee drink containing "sugar" (coffee drink II). Samples were prepared by mixing 1 part of diluted beverage (30 mg sugars/mL) with 2 parts of a stock suspension containing GOx (10 U/mL)/alginate (1.5%)/$CaCO_3$ (30 mM).

As a proof-of-concept we examined the capability of GOx¬mediated gelation to detect glucose in beverage products. Our first example was a comparison of two brands of ice tea: the label for ice tea I reports “HFCS”, whereas the label for ice tea II reports “real sugar”. First, the ice tea was diluted in water to a sugars concentration of 30 mg/mL, and then 1 part of this diluted ice tea was mixed with 2 parts of the stock suspension. After mixing, the vial was left in air for 1 h. As shown in Figure 4.5A, ice tea I induced gel formation consistent with the presence of glucose in the HFCS. Ice tea II was unable to induce gel formation, as expected for this sucrose-containing beverage. The controls (without GOx) did not gel, indicating no contribution of other ingredients in the ice teas to the gel formation

As a second proof-of-concept, we examined two coffee drinks: the label for coffee drink I reports “glucose”, whereas the label for coffee drink II reports “sugar”. The gel-forming experiments were performed as described above. Figure 4.5B shows that glucose-containing coffee drink I induced gel formation, whereas sugar-containing coffee drink II did not induce gel formation. In sum, the test results in Figure 4.5 demonstrate that GOx-mediated alginate gel formation allows a simple and rapid detection of glucose, which may serve as a marker for the presence of a non-sucrose sweetener.

4.4. CONCLUSIONS

In conclusions, we demonstrate a simple and rapid test for glucose-containing sweeteners. This method offers sugar selectivity due to the molecular recognition of the GOx enzyme and transduces recognition into a readily observable mechanical response (i.e., gel formation) that is independent of color in the sample. Furthermore, this method

employs common components (GOx and alginate) that should be safe in the kitchen. Thus, we envision this test could be used on-site by ingredient buyers or in homes, stores, or restaurants. More broadly, this work suggests that emerging research on enzyme-induced gel formation for biomedicine[81-84] may find broader applications in the food industry.

Chapter 5

CELL-MEDIATED GELATION OF AN ALGINATE DERIVATIVE

Chapter Contributions:

The concept of cell gelation using associating polymers was previously demonstrated in our laboratory by Matthew B. Dowling (MBD) using a chitosan derivative. VJ extended this concept to the biocompatible alginate derivative (hm-alginate) discussed in this chapter. The synthesis of hm-alginate as well as the studies of this polymer in conjunction with cells was done by VJ with assistance from Hyuntaek Oh and Feili Huang. Prof. Ian M. White provided guidance for the cell culture and live-dead assays. VJ wrote the chapter, which was critically reviewed by the other authors.

5.1. INTRODUCTION

Biological cells are the building blocks of all organisms. Most cells in complex organisms, however, do not exist as discrete entities – instead, they are usually assembled into functional higher-order structures, *viz*. tissues and organs.[85-90] The connection of cells into tissue is typically mediated by adhesive proteins embedded in neighboring cell membranes. When these connections proliferate across a finite volume, the resulting tissue is a squishy, gel-like material within which the cells are immobilized. Cells in a tissue are typically close-packed into aggregates and these are surrounded by the extracellular matrix (ECM), which is also a gel-like polymeric material

Inspired by the natural assembly of complex biological tissues from cells and ECM, scientists have begun to explore whether cells can be assembled *ex vivo* to create tissue mimics.[87,88] A recent review by Taguchi discusses the growing area of "cellular assembly" and describes various approaches in this regard.[88] It is worth emphasizing that cell assembly is at the heart of biomaterial and tissue engineering. The standard approach in tissue engineering is to culture cells within a polymeric hydrogel. In this case, the cells are passively entrapped as discrete structures in a three-dimensional (3-D) network of polymer chains. Direct connection or contact between adjacent cells occurs only at very high cell densities.

Rather than the above typical case of passively embedding cells in a polymer network, an alternative can be envisioned. That is, a network can be formed in which the *cells serve as active structural elements* (nodes or junctions or crosslinks), with the various nodes being connected (bridged) by polymer chains. In such a scenario, each polymer chain is attached simultaneously to two or more adjacent cells and together these elements build a sample-spanning 3-D network. One example of such cellular assembly was shown by Mooney *et al.*[14] who synthesized a derivative of the polysaccharide alginate with grafted cell-adhesive peptides (containing the RGD, i.e., arginine-glycine-aspartic acid, motif). The polymer chains became bound to cell surfaces via their RGD domains, and the net result was the formation of a network of cells bridged by polymer chains

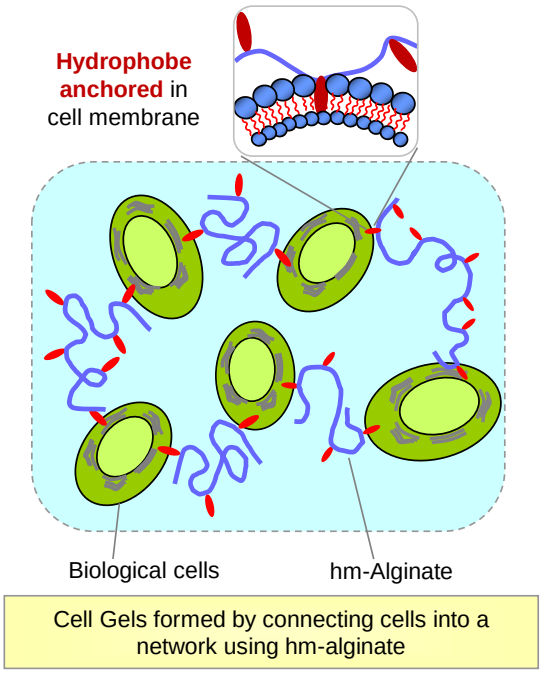

Figure 5.1. Schematic of cell gelation using hydrophobically modified biopolymers. Polymer is shown schematically with its hydrophilic backbone in blue and the grafted hydrophobes in red. Upon addition of polymer to the cells, cells are crosslinked into a three-dimensional network (gel). Gelation is driven by insertion of hydrophobes into cell membranes (as depicted in the top inset); thereby the polymer chains connect (bridge) the cells into a self-supporting network.

More recently, we and others have suggested that cell networking (gelling) can be induced in a simpler manner by hydrophobic interactions. In particular, we synthesized a hydrophobically modified (hm) derivative of the cationic aminopolysaccharide chitosan and combined this polymer with human blood. [91] We showed that hm-chitosan was able to convert a liquid suspension of blood cells into an elastic gel. To explain this gelation, we hypothesized that the polymer chains inserted their hydrophobes into the lipid bilayers of blood cells (due to their mutual hydrophobic affinity) as shown in Figure 5.1. In turn, this resulted in a network with the cells acting as junction points between polymer chains.

In contrast to hm-chitosan, native chitosan (with no hydrophobes) did not cause such gelation.[91]

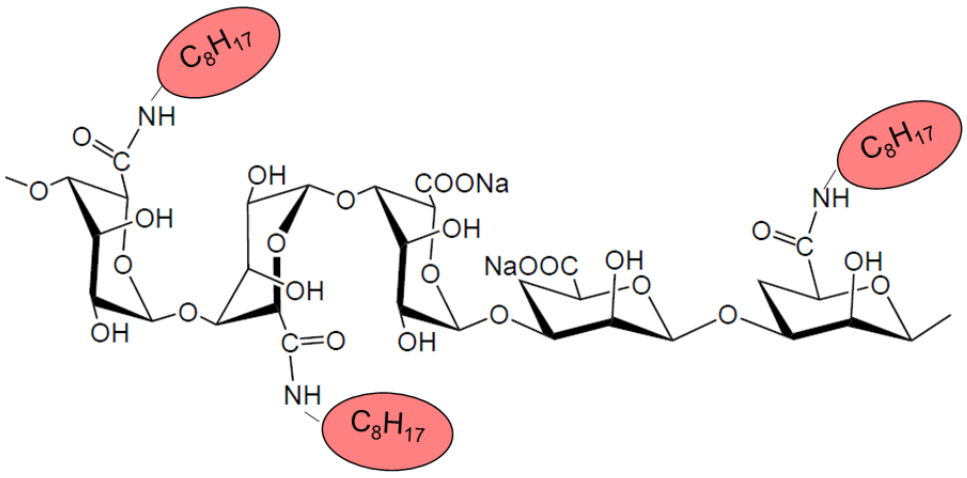

Figure 5.2. Chemical structure of hm-alginate with alkyl hydrophobes.

Based on previous studies, we hypothesize that hydrophobic interactions can be employed in a generic manner for cell gelation, i.e. it neither requires specific cells nor a specific polymer backbone (as long as hydrophobes are grafted to the backbone). The present study seeks to test this hypothesis, i.e., whether this gelation mechanism can be extended to a variety of cells and to different hm-polymers. Towards this end, we have studied several kinds of cells, including human or bovine blood, endothelial cells, and breast cancer cells. We have used a hydrophobically modified derivative of alginate (hm-alginate). We chose alginate because it is a biocompatible and bioresorbable polymer that is widely used in tissue engineering and also as an implantable biomaterial. The chemical structure of hm-alginate is shown in Figure 5.2.

Our results, as shown below, confirm the cell-gelling abilities of hm-polymers. Moreover, in the case of hm-alginate, we have assayed the viability of gelled cells and we find the cells to be mostly viable. We also demonstrate a unique aspect of hm-polymer-mediated gelation of cells, which is that such gelation can be readily reversed by introducing the sugar-based supramolecule α-cyclodextrin (α-CD). This is possible because the hydrophobic interactions that mediate gelation are weak, physical bonds. α-CD has a hydrophobic binding pocket that sequesters the hydrophobes present along the polymer and thereby eliminates the interaction between polymer chains and cells. Overall, cell gelling (networking) by hm-alginate is shown to be a simple, benign process, with its reversibility being an added benefit. This approach could have wide utility, e.g., in biomedical applications such as wound healing, tissue sealing, and for the injectable delivery of cells. In the long term, it could also provide a route towards the directed assembly of cell clusters and tissues.

5.2. EXPERIMENTAL SECTION

Materials. The polymer alginate was obtained from Sigma-Aldrich. Sodium alginate (product number A2033, from brown algae) had a molecular weight of 80,000–120,000. The following chemicals were also purchased from Sigma-Aldrich: *n*-octylamine, and N-(3-dimethylamino-propyl)-N′-ethylcarbodiimide hydrochloride (EDC). The supra-molecule α-cyclodextrin (α-CD) was obtained from TCI. Heparanized bovine blood was purchased from Lampire. Human umbilical vein endothelial cells (HUVEC) (product number: C2517A) was purchased from Lonza. Breast cancer cells (MCF7) were purchased from ATCC. MCF7 cell culture reagents: Dulbecco's modified eagle medium

(DMEM) containing high glucose, fetal bovine serum, pencilin, streptomycin, and trypsin-EDTA) were purchased from ThermoScientific. HUVEC cell culture reagents: endothelial growth media (EGM-2) and supplement EGM-2 bulletkit were purchased from Lonza. Live/Dead® assay kit for mammalian cells was purchased from Invitrogen. All chemicals and materials were used as received without further purification.

Hydrophobically Modified Alginate (hm-alginate) Synthesis. hm-alginate with C_8 hydrophobes was synthesized by an amidation reaction with *n*-octylamine using EDC as the coupling reagent. The synthesis procedure was same as that described by Nystrom et al.[2] The product was precipitated by adding acetone and separated by vacuum filtration. This purification step was repeated 5 times. The final product was recovered by vacuum drying at room temperature. The degree of hydrophobic modification was determined by ^{1}H-NMR as described previously.[92] ^{1}H NMR spectra were taken on a Bruker AVANCE 500MHZ spectrometer. Spectra were referenced to the 3-trimethylsilypropionic acid sodium salt-d4. The calculated degree of hydrophobic modification was 25 mol% of uronic acid residues in the alginate chains.

Cell Culture and Cell Gelation. For culture of MCF7 cells, high-glucose DMEM media supplemented with 5μL/mL of penicillin or streptomycin and 10% fetal bovine serum (FBS) was used. For HUVEC cells, EGM-2 media was first completed with EGM-2 bulletkit (containing hydrocortisone, gentamicin or amphotericin-B, fetal bovine serum, growth factors, ascorbic acid, and heparin). Both cells were cultured separately in T75 flasks in a 37°C incubator with 5% CO_2. Cells were subcultured every 5-7 days by

trypsinization with 0.25%/0.02% trypsin/EDTA. To prepare cells for gelation experiments, confluent cells were harvested from the T75 flask, centrifuged to a pellet and re-suspended in 0.5 mL of cell growth media. Cell gelation was studied by adding stock solutions of the corresponding polymer to the above cell suspension, followed by slow mixing. In the case of alginate and hm-alginate, the polymers were dissolved in PBS. In all cases, 0.9 wt% NaCl was added to the solutions for osmotic balance

Rheological Studies. A TA Instruments AR2000 stress-controlled rheometer was used to perform steady and dynamic rheological experiments. All experiments were done at 25°C using a cone-and-plate geometry (40 mm diameter and 2° cone angle). A solvent trap was used to minimize drying of the sample during measurements. Dynamic frequency spectra were conducted in the linear viscoelastic regime of the samples, as determined by prior dynamic strain sweeps.

Cyclodextrin Gel Reversal. A stock solution of 10 wt% α-CD was prepared in deionized (DI) water and a small volume (200 μL) of this solution was added to 2 mL of the cell containing gel, followed by vortex mixing. Adding just a small volume of the α-CD solution ensured that the gel was negligibly diluted in the process.

Live-Dead Assay. A solution containing 4 μM of live (calcien-AM) and dead (ethidium homodimer) assay reagent was prepared in PBS. To stain the cells, 10 μL of this solution was added to the cell-gel, incubated at room temperature for 15 min and then imaged on a confocal microscope (Leica SP5 X). For imaging calcein-AM, the excitation was done at

495 nm and emitted light was recorded using a 505–554 nm band-pass filter. For imaging ethidium homodimer, the excitation was done at 556 nm and imaging was done with a 568-700 nm band pass filter. Cells were imaged within successive optical slices of 1.3 μm thickness to visualize live cells (stained green) and dead cells (stained red) along different planes of the sample. Projections of these images along the XY plane (top view) and XZ plane (cross-sectional view) were then constructed using the Leica Application Suite. All images were obtained within 1 h of sample preparation.

5.3. RESULTS AND DISCUSSION

Cell Gelation with hm-Alginate

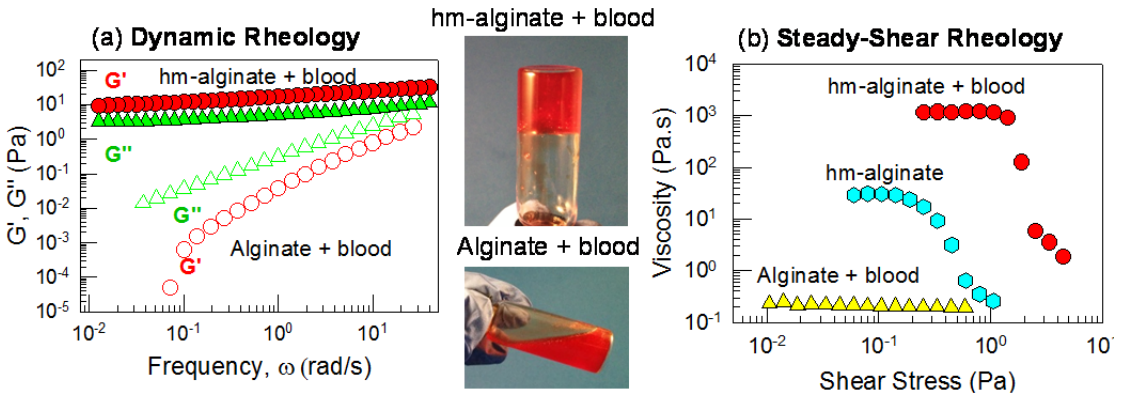

Figure 5.3. Effect of 0.93 wt% of hm-alginate or alginate on heparinized bovine blood. The photographs show that the hm-alginate/blood mixture (Photo1) is a self-supporting gel that holds its weight in the inverted vial whereas the alginate/blood mixture (Photo2) is a freely flowing liquid. In (a) dynamic of both samples is shown. The hm-alginate sample (closed symbols) displays the rheology of a physical gel (G'>G'') whereas the alginate sample (open symbols) responds like a viscous sol. In (b) Steady-shear rheological data for the viscosity vs. shear stress are shown. The hm-alginate/blood mixture (red circles) show a significantly higher viscosity relative to both the alginate/blood mixture (yellow triangles) as well as a 0.93 wt% solution of hm-alginate with no blood (cyan hexagons).

We explored cell gelation using hm-alginate (having C_8 hydrophobes). One advantage of alginate derivatives including hm-alginate is that they can be dissolved in water at neutral pH. Our initial studies were done with heparinized bovine blood; note that the heparin ensures that the blood will not undergo the natural clotting cascade. To this blood, we added a solution of hm-alginate so that the concentration of polymer in the overall sample was 0.93 wt%. For comparison, a second sample was made by combining blood with an identical concentration of the parent alginate polymer. The mixture of hm-alginate and blood quickly formed a gel that supported its weight in the inverted vial, as

shown by Photo 1 in Figure 5.3. In contrast, the mixture of alginate and blood remained a freely flowing liquid (similar to the blood alone), as indicated by Photo 2 in Figure 5.3.

Rheological data confirm the differences between the above samples. Figure 5.3a presents data from dynamic rheology. The hm-alginate/blood sample shows the rheological signature of a weak gel, i.e., $G' > G''$ over the frequency range, with both moduli showing negligible variation with frequency. On the other hand, the alginate/blood sample exhibits a viscous response: both moduli vary sharply with frequency and $G'' > G'$ at all frequencies. Next, Figure 5.3b presents data from steady-shear rheology on the same samples. Here, the apparent viscosity is plotted as a function of shear stress. The alginate/blood sample displays a constant viscosity of ~ 0.2 Pa.s (Newtonian response). In contrast, the hm-alginate/blood sample shows a shear-thinning (non-Newtonian) response, with a high viscosity at low shear-stresses followed by a decrease in viscosity at higher shear stresses. The zero-shear viscosity, i.e., the viscosity in the low-shear limit, is ~1000 Pa.s, which is four orders of magnitude higher than that of the alginate/blood sample. The steep drop in viscosity around a stress of 2 Pa is indicative of a yield stress in the material, i.e., the sample flows negligibly at stresses below this value, consistent with its ability to hold its weight under vial inversion. Also, it should be noted that 0.93 wt% hm-alginate alone (without blood) is not a gel; rather its rheological profile (Figure 5.3b) is indicative of a viscous liquid with moderate shear-thinning. The above data show that gelation of blood can be induced by hm-alginate (but not native alginate). Once again, this implies a cell network bridged by hm-alginate

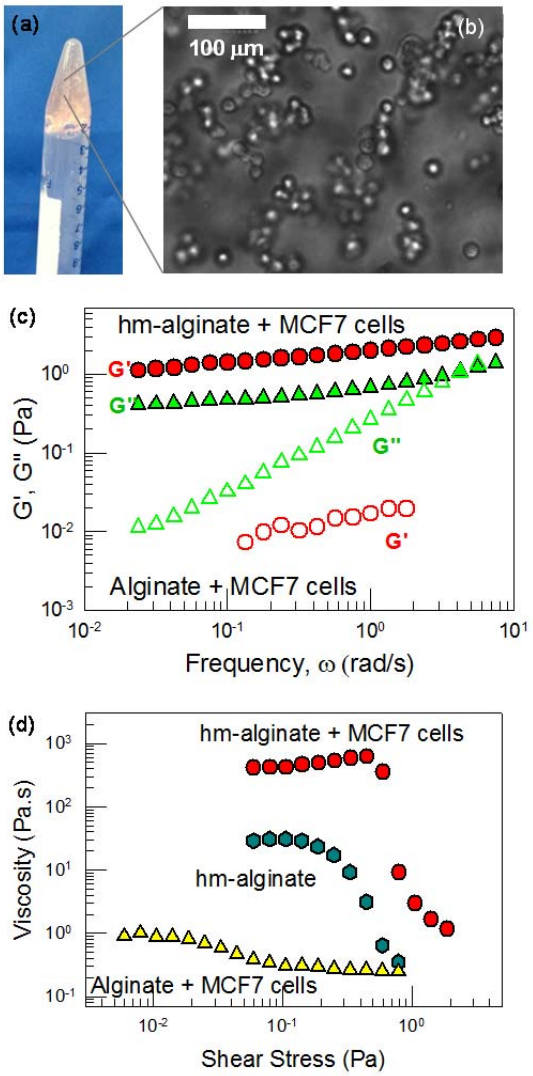

Figure 5.4. Effect of 0.93 wt% of hm-alginate or alginate on heparinized bovine blood. (a)The photographs show that the hm-alginate/blood mixture (Photo1) is a self-supporting gel that holds its weight in the inverted vial whereas (b) the alginate/blood mixture (Photo2) is a freely flowing liquid. In (c) dynamic of both samples is shown. The hm-alginate sample (closed symbols) displays the rheology of a physical gel (G'>G'') whereas the alginate sample (open symbols) responds like a viscous sol. In (d) Steady-shear rheological data for the viscosity vs. shear stress are shown. The hm-alginate/blood mixture (red circles) show a significantly higher viscosity relative to both the alginate/blood mixture (yellow triangles) as well as a 0.93 wt% solution of hm-alginate ith no blood (cyan hexagons).

chains, with the driving force being the affinity between the hydrophobes on the polymer and cellular bilayers (Figure 5.1).

To demonstrate the ability of hm-alginate to gel a variety of cells, we tested two cell types, HUVECs and mammalian breast cancer cells (MCF7). Hm-alginate was able to gel both types of cells and results are shown below for MCF7. Initially, a freely flowing suspension of MCF7 cells (4.6×10^7 cells/mL) was placed in a tube. A solution of hm-alginate in PBS was added to achieve an overall concentration of 0.93 wt% polymer. Upon addition of hm-alginate, the cell suspension was transformed into a gel that did not flow in the inverted tube, as can be seen from the photograph in Figure 5.4a. When this gel was observed under optical microscopy, clusters of cells could be seen (Figure 5.4b). In contrast, a mixture of MCF7 cells with the native alginate (at identical concentrations of cells and polymer) remained a freely flowing liquid. Dynamic rheological data (Figure 5.4c) again confirm the differences between MCF7 samples containing hm-alginate and alginate. The former shows the signature of a gel ($G' > G''$, both nearly independent of frequency) whereas the latter shows the response of a viscous liquid ($G'' > G'$, both varying with frequency). Thus, our results confirm the ability of hm-alginate to act as a generic gelator for various cells, similar to hm-chitosan. By extension, we expect other hydrophobically modified biopolymers to also be capable of inducing cell gelation by an identical mechanism.

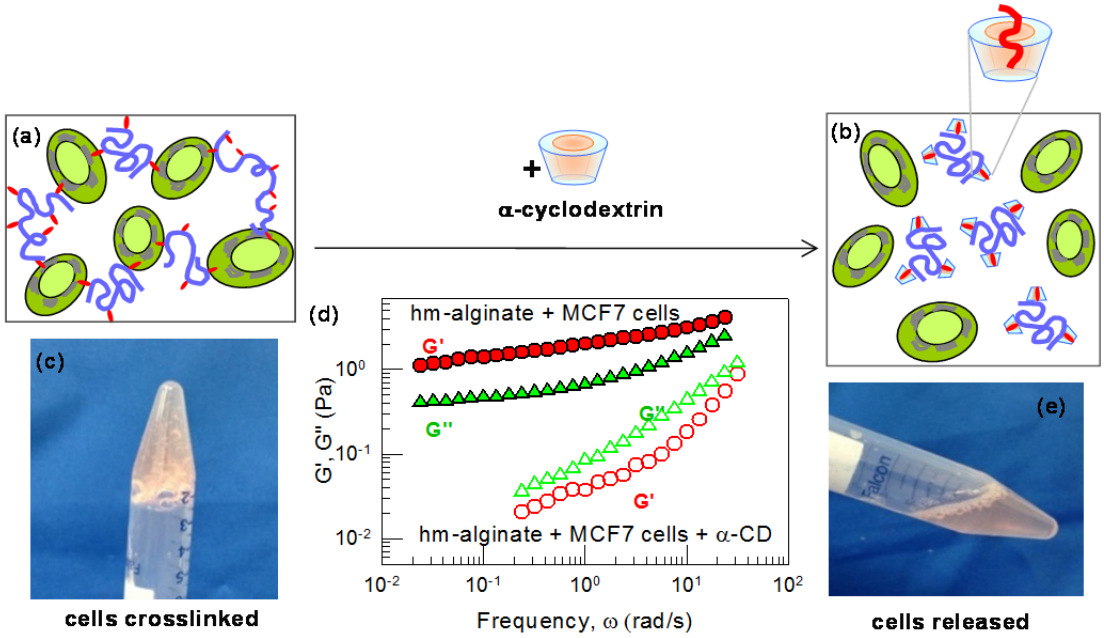

Figure 5.5. Reversal of MCF7 cell gelation by α- cyclodextrin (α-CD). (a & b) The top schematic illustrates the mechanism for this reversal. The α-CD molecule has a barrel shape with an inner hydrophobic pocket. When added to a hm-chitosan/MCF7 cell gel, the polymer hydrophobes unhook from the cells and instead get buried within the hydrophobic pockets of α-CDs. The connection between the cells are thus eliminated and the gel is liquefied releasing (or harvesting) previously entrapped cells. (c) Photograph (Photo1) of hm-alginate/MCF7 cell gel before the addition of α-CD. In (d) dynamic rheology data of hm-alginate cells gel before and after the addition of α-CD. Sample without α-CD shows a gel-like response whereas the sample containing α-CD shows a viscous response. (e) Photograph (Photo2) of hm-alginte/MCF7 cell gel after addition of α-CD showing the freely flowing sample.

A distinct advantage of cell gelation by hm-polymers is that it is based on weak, non-covalent interactions and hence can be reversed by addition of species with hydrophobic binding pockets. We demonstrate this now for the case of MCF7 cells gelled by hm-alginate. To the gel from Figure 5.4, we add the sugar-based supramolecule α-cyclodextrin (α-CD) at a concentration of 0.91 wt%. As shown in Figure 5.5, the gel (Figure 5.5c) is immediately transformed into a freely flowing liquid (Fgure 5.5e). This result is corroborated by dynamic rheology (Figure 5.5d). The initial sample has a gel-

like response whereas, after addition of α-CD, the sample shows a viscous response ($G'' > G'$, both varying with frequency). The mechanism for the reversal of gelation is shown by the schematics in Figure 5.5a and 5.5b. Initially, the hydrophobes (red tails) along the polymer chains are embedded in cell membranes. When the α-CD is added, the hydrophobic tails instead become sequestered within the hydrophobic binding pockets of α-CD molecules (shown in orange). The polymer chains are thus prevented from interacting with the cell membranes. In turn, because the cells are no longer bridged by polymer chains, the gel is converted to a liquid, i.e., the cells are released. Note that the ability to reverse gelation through α-CD further substantiates the fact that hydrophobic interactions are responsible for the gelation in the first place. Similar results on reversal of gelation were observed in all the cases mentioned above, i.e., regardless of cell type or the type of hm-polymer. We should also note that the size of the binding pocket in α-CD is such that it effectively binds the single-tailed hydrophobes on our hm-polymers; however, it is not large enough to bind the twin-tails on lipids that constitute cell membranes. Thus, the use of α-CD to reverse cell-gels constitutes a simple, benign, and biocompatible approach.

Viability of Cells in Cell-Gels

A key remaining question is the fate of the cells within a cell gel, i.e., do the cells continue to remain viable even as they serve as the nodes in a 3-D polymer-bridged network? To assess the effect of gelation on cell viability, we performed live-dead assays on hm-alginate-MCF7 cell-gels (composition identical to that in Figures 5.4, 5.5). Calcein-AM was used as the live stain and ethidium homodimer as the dead stain.

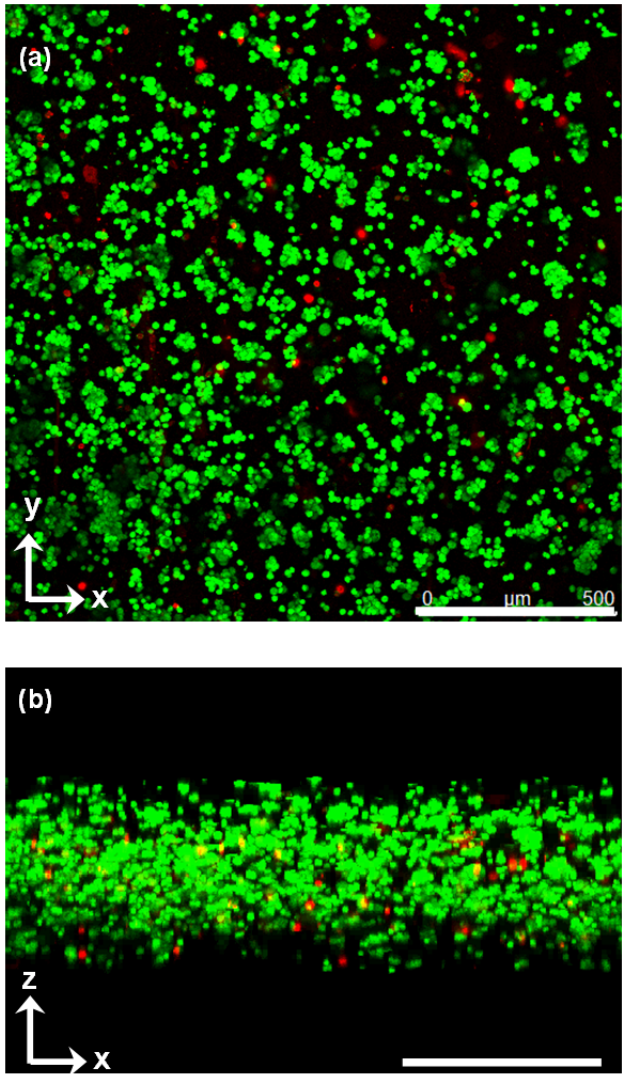

Figure 5.6. Confocal microscope data showing live-dead assay of hm-alginate/ MCF7 cell gels. Three-dimensional gel was imaged in various optical sections and the data is presented. (a) Top view of projection of various optical sections of the gel on XY plane. A large population of the cells were alive (stained green) with only a few cells dead (stained red) (b) Side view (vertical cross-section) of the three-dimensional gel showing cells held in multiple planes (presumably by hm-alginate) and majority of them were still alive. These results confirm that cell-gelation process with hm-alginate is benign to cells.

Following exposure of cells to these stains, confocal microscopy was used to monitor the resulting fluorescence. A green fluorescence due to calecin is indicative of live cells whereas red fluorescence due to intercalation of ethidium is indicative of dead cells. Figure 5.6a shows a projection of multiple optical sections captured at different heights of the cell gel. Figure 5.6b shows a projection of the same images on the XZ plane. The images reflect a superposition of both green and red fluorescence. We find that the vast majority of the cells are stained green whereas only a few cells are stained red. This demonstrates that gelation of MCF7 cells by hm-alginate is benign to the cells. The images also indicate the presence of a 3-D network of cells throughout the sample. Although more extensive studies on cell viability need to be conducted, our initial results do suggest that cell gelation by hm-polymers is a benign process. The ability to form gels of cells in this manner by self-assembly (and also to reverse the gelation, on demand) could prove to be useful in biomedical engineering. For example, cell-gels could serve as injectable biomaterials. The shear-thinning property of cell-gels (see Figure 5.3) should allow them to be injectable by a syringe. Once the gel is ejected from the tip of the syringe needle, it quickly reforms and reverts to its initial gel state, which ensures that the gel will remain localized at the site of injection.

4.4. CONCLUSIONS

We have shown that a variety of cells can be gelled by hm-alginate. These hydrophilic biopolymers with hydrophobic grafts attached along their backbone have the ability to transform freely flowing cell suspensions into elastic gels. The gelling mechanism is based on the insertion of hydrophobes on the polymers into the lipid-rich

cellular membrane) and therby bridging the cells into a physical 3-dimensional network. This cell gelation occurs without the need of an external crosslinking reagent because the functional component (cells) also serve as active structural components (nodes or crosslinking junction points) in the network formation rather than being passively entrapped in a polymeric mesh. An additional and unique advantage of cell gelation with hm-polymers are that the cells can be recovered from the gel by addition of a supramolecule a-CD,without the need of enzymes or harsh chemicals). Furthermore, the process of cell-gelation with hm-alginate is benign to cells, as demonstrated by live-dead cell assay. Owing to the generality of the hydrophobe and cell-membrane interactions, we envision that this gelation mechanism can be extended to other hydrophobically modified biopolymers to gel a variety of cells. Thus, hm-polymers for cell-gelation may find several significant biological applications, e.g. 3D cell culture, injectable cell gels (for cellular therapy), tissue sealants and other tissue engineering applications.

Chapter 6

CONCLUSIONS AND RECOMMENDATIONS

6.1. Project Summary and Principal Contributions

In this dissertation, we have shown three new concepts for stimuli-responsive gelation of alginate and its derivatives to impart new structural and functional properties which were unavailable in conventional alginate gels. Gelation response of alginate was extended to the following stimuli: (1) Light (by using PAG and $CaCO_3$); (2) Enzymes (by using glucose oxidase/glucose and $CaCO_3$); and (3) Biological stimuli (by using hydrophobes and cells).

In chapter 3, we demonstrated light responsive gelation of alginate. The components of the system were alginate/$CaCO_3$/PAG. Upon exposure to UV light, the PAG gets photolyzed and thereby releases H^+ ions, which react with $CaCO_3$ to form soluble Ca^{2+} ions. Alginate cross-links in the presence of calcium ions to form Ca-alginate hydrogel. Thus light responsiveness is imparted to alginate/$CaCO_3$ mixtures by combining it with PAG.

In chapter 4, we demonstrated enzymatic gelation of alginate in response to addition of glucose. The components of the system were alginate/$CaCO_3$ and glucose/glucose oxidase. Glucose gets oxidized by GOx to generate H^+ ions which then generate free Ca^{2+} ions *in-situ*. Ca^{2+} ions then crosslink alginate to form a Ca-alginate gel. Thus enzyme responsiveness and response to small molecule stimuli are imparted to alginate/$CaCO_3$ mixture by addition of glucose/glucose oxidase.

In chapter 5, we demonstrate gelation of hm-alginate mediated by cells. The cross-links in this system are based on hydrophobic interactions (unlike ionic interactions in chapter 3,4). Alginate is made cell-responsive by grafting hydrophobes onto its backbone which are known to interact (and insert) into the lipid bilayers of cells. Upon addition of cells to hm-alginate, cells facilitate insertion of hydrophobes from different polymer chains and thereby serve as crosslinking junction for various polymer chains. Gelation occurs due to formation of a 3D network of polymers cross-linked by cells. Thus, cell-responsiveness is imparted to alginate by addition of hydrophobes and cells to hm-alginate solution.

In addition to proving these concepts, we further demonstrated that these concepts can be used to impart structure (spatially selective microscale patterns) or function (sensing, hemostatic, therapeutic) to alginate hydrogels. Light-responsive gelation enlists the structural capability of building photopatterned erasable hydrogels. Enzymatic gelation enlists the functional capability of sensing (glucose detection). Cell-mediated gelation enlists the functional capability to create tissue engineering matrices.

6.2. RECOMMENDATIONS FOR FUTURE WORK

Based on the concepts that we have reported in this dissertation, it is highly possible to explore and envision new possibilities following the platforms and expertise that we have developed. Here, we briefly describe the outline for future work.

6.2.1. Light-Activated Ionic Gelation of Alginate

In chapter 3, we described a simple approach for gelation of photogelation of alginate. In the future, we will continue to do more studies on this system to improving its performance by decreasing the time of UV exposure required to form the gel. In principle, this can be achieved by increasing the clarity (or UV transparency) of the pre-gel solution. We have identified that the transparency can be improving by replacing insoluble calcium carbonate particles in the pre-gel with soluble calcium vectors like disodium calcium ethylenediaminetetraacetate. Another possible solution to improve the clarity is to introduce an additional component in the pre-gel solution which can absorb (or sequester) the hydrophobic byproducts of photolyzed PAG. α-CD, which was used in chapter 4 to sequester the hydrophobe, can be used in this context to sequester these hydrophobic byproducts and improve the clarity.

In addition to improving the efficiency of the system, we can also envision using this photogelation approach for other applications. This system can have potential application as: (i) Microfuidic valve; (ii) Bio-photoresist; and (iii) Three-dimensional (3D) soft materials fabrication.

Microfluidic Valve. In chapter 3, we have shown the ability to photopattern hydrogels on a flat substrate by smearing the pre-gel on the substrate. Alternately, if the pre-gel solution is flowing through a microfluidic device, a section of the microfluidic channel can be gelled by UV irridiation through a photomask. This gel in the microfluidic channel can act a valve to block the flow through that channel and direct it into other channels. This method has a unique advantage that it can be unblocked by simply flowing a solution containing calcium chelators to dissolve the photogel.

Bio-photoresist. In chapter 3, for the photopatterning studies, we have used the matrix of the patterned hydrogel to entrap and release components of interest on-demand. Alternately, we can also use the matrix as a barrier to chemicals or small biomolecules trying to react with the substrate. This barrier property enables us to use it as a biophotoresist. For example, Figure 6.1 shows spatial patterning of green fluorescent molecule on chitosan coated glass slide using photopatterned alginate as the photoresist. By direct reaction (route 1 in Figure 6.1) of NHS-flourescein (green fluorescent molecule) with chitosan casted on a glass slide, it yields a fluorescent chitosan film in which all the chitosan has reacted with NHS-fluorescein. However, it becomes very hard if we want only specific areas of chitosan to react (and not the other areas). By using photopatterned alginate as a photoresist, we can overcome this limitation. As shown in route 2 of Figure 6.1, specific areas on chitosan can be reacted with NHS-fluorescein if we follow the following steps sequentially: (i) Photopatterning of alginate hydrogel on chitosan casted glass slide(as shown in photograph in Figure 6.1). (ii) Reacting this substrate (containing alginate on top of chitosan casted glass slide) with NHS-flourescein.

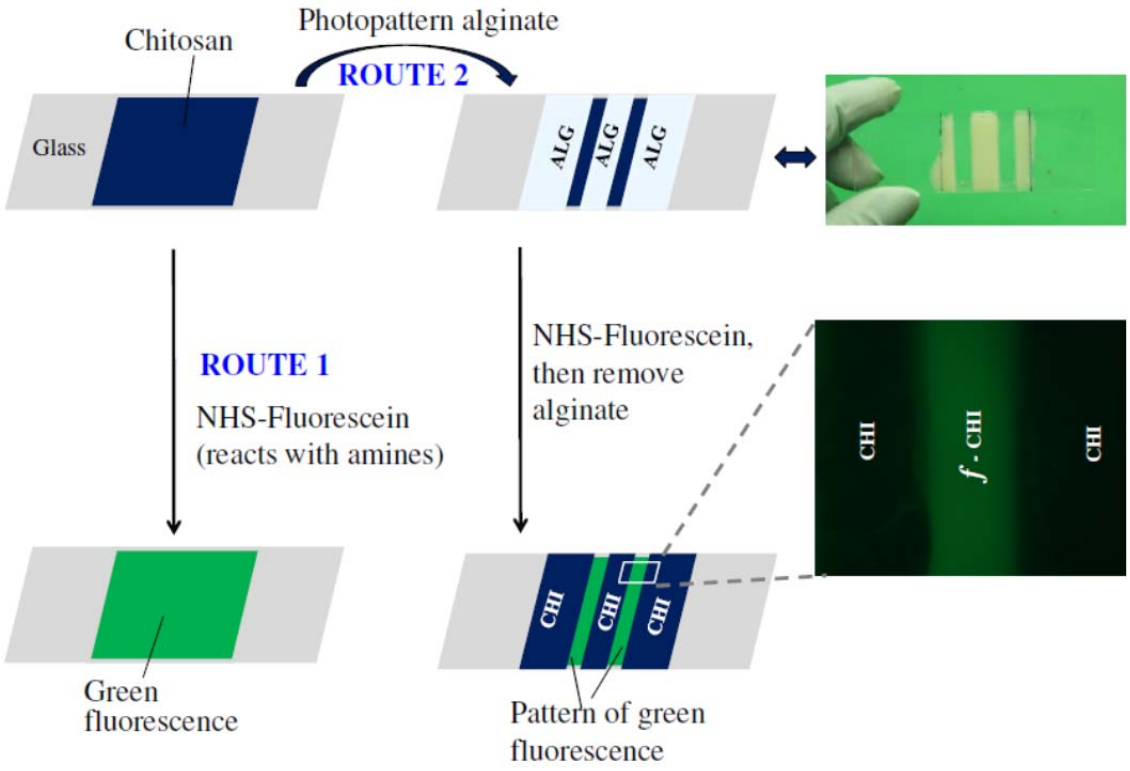

Figure 6.1. Photopatterning of alginate hydrogel on a chitosan coated glass and using it as a sacrificial biophotoresist to pattern molecules of interest on a reactive chitosan substrate.

(iii) Then removing the alginate using calcium chelator. These steps yield a chitosan film with fluorescein reacted on only specific areas of chitosan (as shown in fluorescent micrograph in Figure 6.1. Thus by using photogelling alginate as a photoresist, we can achieve the capability of patterning molecules on substrates. Patterning of NHS-fluorescein on chitosan casted glass slide is shown here as a proof-of-concept demonstration but in principle it can be used to pattern sensitive proteins, antibodies, etc. It should be noted that harsh conditions used in conventional photoresists might denature (or damage) these sensitive biomolecules of interest.

3D Soft-material Fabrication. The concept of photogelation and two-dimensional (2D) photopatterning can be extended to fabricate three-dimensional (3D) soft materials. The concepts of stereolithography can be used to achieve bottom-up fabrication by sequentially building patterned layers of 2D features on top of previously patterned layers (layer-by-layer fashion). Alternately, 3D spatial selectivity (and precision) of two-photon lithography can also be used to construct 3D soft-materials using photogelation of alginate. It is to be noted that the advantage of these 3D structures is that they can be chemically erased under mild conditions.

6.2.2. Enzymatic Gelation of Alginate. In chapter 4, glucose detection was achieved by exploiting the substrate specificity of glucose oxidase to recognize glucose. In principle, detection can be extended to other sugars by first converting the test sugar into glucose (by using sugar specific enzymatic reactions) and then detecting the *in-situ* generated glucose with the procedure as explained in Chapter 4. For example, if the test sugar is sucrose, it can first be converted to glucose and fructose using invertase enzyme. The glucose generated can then be recognized by glucose oxidase and it can be transduced into visual result (sol-gel transition) using alginate/$CaCO_3$ mixture.

6.2.3. Cell-Mediated Gelation of an Alginate Derivate

In chapter 5, we have demonstrated that hm-alginate can be used to gel a variety of cells. As an initial step towards potential applications, we proved that the gelation is benign to cells. In the future, we are expecting to perform systematic studies on growth (3D cell culture) of entrapped cells (HUVECs and MCF7). As hm-alginate is cell-

interactive, we believe that 3D culture of cells in hm-alginate matrix might be similar to cell growth in natural extracellular matrix.

In chapter 5, we mentioned that the capability of gelation of blood cells with hm-alginate will have application as hemostatic materials. As a part of future work, we are expecting to study the properties of hm-alginate/blood gels by varying hydrophobic character (% modification, length of hydrophobe). We also plan to perform *in-vivo* animal tests to confirm the hemostatic ability of hm-alginates.

.

REFERENCES

[1] Kang, H. A.; Shin, M. S.; Yang, J. W. "Preparation and characterization of hydrophobically modified alginate." *Polymer Bulletin* **2002**, *47*, 429-435.

[2] Galant, C.; Kjoniksen, A. L.; Nguyen, G. T. M.; Knudsen, K. D.; Nystrom, B. "Altering associations in aqueous solutions of a hydrophobically modified alginate in the presence of beta-cyclodextrin monomers." *Journal of Physical Chemistry B* **2006**, *110*, 190-195.

[3] Ghahramanpoor, M. K.; Najafabadi, S. A. H.; Abdouss, M.; Bagheri, F.; Eslaminejad, M. B. "A hydrophobically-modified alginate gel system: utility in the repair of articular cartilage defects." *Journal of Materials Science-Materials in Medicine* **2011**, *22*, 2365-2375.

[4] Drury, J. L.; Mooney, D. J. "Hydrogels for tissue engineering: scaffold design variables and applications." *Biomaterials* **2003**, *24*, 4337-4351.

[5] Lee, K. Y.; Mooney, D. J. "Hydrogels for tissue engineering." *Chemical Reviews* **2001**, *101*, 1869-1879.

[6] Augst, A. D.; Kong, H. J.; Mooney, D. J. "Alginate hydrogels as biomaterials." *Macromolecular Bioscience* **2006**, *6*, 623-633.

[7] Kuo, C. K.; Ma, P. X. "Ionically crosslinked alginate hydrogels as scaffolds for tissue engineering: Part 1. Structure, gelation rate and mechanical properties." *Biomaterials* **2001**, *22*, 511-521.

[8] Jeon, O.; Bouhadir, K. H.; Mansour, J. M.; Alsberg, E. "Photocrosslinked alginate hydrogels with tunable biodegradation rates and mechanical properties." *Biomaterials* **2009**, *30*, 2724-2734.

[9] Chueh, B. H.; Zheng, Y.; Torisawa, Y. S.; Hsiao, A. Y.; Ge, C. X.; Hsiong, S.; Huebsch, N.; Franceschi, R.; Mooney, D. J.; Takayama, S. "Patterning alginate hydrogels using light-directed release of caged calcium in a microfluidic device." *Biomedical Microdevices* **2010**, *12*, 145-151.

[10] Shi, X. W.; Tsao, C. Y.; Yang, X. H.; Liu, Y.; Dykstra, P.; Rubloff, G. W.; Ghodssi, R.; Bentley, W. E.; Payne, G. F. "Electroaddressing of Cell Populations by Co-Deposition with Calcium Alginate Hydrogels." *Advanced Functional Materials* **2009**, *19*, 2074-2080.

[11] Huang, S. H.; Hsueh, H. J.; Jiang, Y. L. "Light-addressable electrodeposition of cell-encapsulated alginate hydrogels for a cellular microarray using a digital micromirror device." *Biomicrofluidics* **2011**, *5*.

[12] Westhaus, E.; Messersmith, P. B. "Triggered release of calcium from lipid vesicles: a bioinspired strategy for rapid gelation of polysaccharide and protein hydrogels." *Biomaterials* **2001**, *22*, 453-462.

[13] Sakai, S.; Kawakami, K. "Synthesis and characterization of both ionically and enzymatically cross-linkable alginate." *Acta Biomaterialia* **2007**, *3*, 495-501.

[14] Lee, K. Y.; Kong, H. J.; Larson, R. G.; Mooney, D. J. "Hydrogel formation via cell crosslinking." *Advanced Materials* **2003**, *15*, 1828-1832.

[15] Raeburn, J.; McDonald, T. O.; Adams, D. J. "Dipeptide hydrogelation triggered via ultraviolet light." *Chemical Communications* **2012**, *48*, 9355-9357.

[16] Pawar, S. N.; Edgar, K. J. "Alginate derivatization: A review of chemistry, properties and applications." *Biomaterials* **2012**, *33*, 3279-3305.

[17] Fang, Y. P.; Al-Assaf, S.; Phillips, G. O.; Nishinari, K.; Funami, T.; Williams, P. A. "Binding behavior of calcium to polyuronates: Comparison of pectin with alginate." *Carbohydrate Polymers* **2008**, *72*, 334-341.

[18] Sikorski, P.; Mo, F.; Skjak-Braek, G.; Stokke, B. T. "Evidence for egg-box-compatible interactions in calcium-alginate gels from fiber X-ray diffraction." *Biomacromolecules* **2007**, *8*, 2098-2103.

[19] Tsugio, K. Photochemistry of Hypervalent Iodine Compounds. In *CRC Handbookof Organic Photochemistry and Photobiology, Volumes 1 & 2, Second Edition*; CRC Press, 2003.

[20] Bankar, S. B.; Bule, M. V.; Singhal, R. S.; Ananthanarayan, L. "Glucose oxidase - An overview." *Biotechnology Advances* **2009**, *27*, 489-501.

[21] Szejtli, J. "Introduction and general overview of cyclodextrin chemistry." *Chemical Reviews* **1998**, *98*, 1743-1753.

[22] Abdala, A. A.; Tonelli, A. E.; Khan, S. A. "Modulation of hydrophobic interactions in associative polymers using inclusion compounds and surfactants." *Macromolecules* **2003**, *36*, 7833-7841.

[23] Burckbuchler, V.; Kjoniksen, A. L.; Galant, C.; Lund, R.; Amiel, C.; Knudsen, K. D.; Nystrom, B. "Rheological and structural characterization of the interactions between cyclodextrin compounds and hydrophobically modified alginate." *Biomacromolecules* **2006**, *7*, 1871-1878.

[24] Karlson, L.; Thuresson, K.; Lindman, B. "Cyclodextrins in hydrophobically modified poly(ethylene glycol) solutions: Inhibition of polymer-polymer associations." *Langmuir* **2002**, *18*, 9028-9034.

[25] Liao, D.; Dai, S.; Tam, K. C. "Rheological properties of hydrophobic ethoxylated urethane (HEUR) in the presence of methylated beta-cyclodextrin." *Polymer* **2004**, *45*, 8339-8348.

[26] Tonelli, A. E. "Nanostructuring and functionalizing polymers with cyclodextrins." *Polymer* **2008**, *49*, 1725-1736.

[27] Macosko, C. W.ㅌ Rheology principles, measurements, and applications.ㅓ **1994**.

[28] Foster. In *Optimizing Light Microscopy for Biological & Clinical Labs* Kendall/Hunt Publishing Company: Dubuque, 1997.

[29] Spencer, M. *Fundamentals of light microscopy*; Cambridge University Press: Cambridge [Cambridgeshire]; New York, 1982.

[30] Suzuki, A.; Tanaka, T. "Phase-transition in polymer gels induced by visible light." *Nature* **1990**, *346*, 345-347.

[31] Eastoe, J.; Vesperinas, A. "Self-assembly of light-sensitive sufactants." *Soft Matter* **2005**, *1*, 338-347.

[32] de Jong, J. J. D.; Hania, P. R.; Pagzlys, A.; Lucas, L. N.; de Loos, M.; Kellogg, R. M.; Feringa, B. L.; Duppen, K.; van Esch, J. H. "Light-driven dynamic pattern formation." *Angewandte Chemie-International Edition* **2005**, *44*, 2373-2376.

[33] Kumar, N. S. S.; Varghese, S.; Narayan, G.; Das, S. "Hierarchical self-assembly of donor-acceptor-substituted butadiene amphiphiles into photoresponsive vesicles and gels." *Angewandte Chemie-International Edition* **2006**, *45*, 6317-6321.

[34] Matsumoto, S.; Yamaguchi, S.; Ueno, S.; Komatsu, H.; Ikeda, M.; Ishizuka, K.; Iko, Y.; Tabata, K. V.; Aoki, H.; Ito, S.; Noji, H.; Hamachi, I. "Photo gel-sol/sol-gel transition and its patterning of a supramolecular hydrogel as stimuli-responsive biomaterials." *Chemistry-a European Journal* **2008**, *14*, 3977-3986.

[35] Kloxin, A. M.; Kasko, A. M.; Salinas, C. N.; Anseth, K. S. "Photodegradable hydrogels for dynamic tuning of physical and chemical properties." *Science* **2009**, *324*, 59-63.

[36] Wolff, T.; Emming, C. S.; Suck, T. A.; Von Bunau, G. "Photorheological effects in micellar solutions containing anthracene derivatives - a rheological and static low-angle light-scattering study." *Journal of Physical Chemistry* **1989**, *93*, 4894-4898.

[37] Ketner, A. M.; Kumar, R.; Davies, T. S.; Elder, P. W.; Raghavan, S. R. "A simple class of photorheological fluids: Surfactant solutions with viscosity tunable by light." *Journal of the American Chemical Society* **2007**, *129*, 1553-1559.

[38] Kumar, R.; Raghavan, S. R. "Photogelling fluids based on light-activated growth of zwitterionic wormlike micelles." *Soft Matter* **2009**, *5*, 797-803.

[39] Kumar, R.; Ketner, A. M.; Raghavan, S. R. "Nonaqueous photorheological fluids based on light-responsive reverse wormlike micelles." *Langmuir* **2010**, *26*, 5405-5411.

[40] Sun, K. S.; Kumar, R.; Falvey, D. E.; Raghavan, S. R. "Photogelling colloidal dispersions based on light-activated assembly of nanoparticles." *Journal of the American Chemical Society* **2009**, *131*, 7135-7141.

[41] Sakai, H.; Orihara, Y.; Kodashima, H.; Matsumura, A.; Ohkubo, T.; Tsuchiya, K.; Abe, M. "Photoinduced reversible change of fluid viscosity." *Journal of the American Chemical Society* **2005**, *127*, 13454-13455.

[42] Dektar, J. L.; Hacker, N. P. "Photochemistry of diaryliodonium salts." *Journal of Organic Chemistry* **1990**, *55*, 639-647.

[43] Reichmanis, E.; Houlihan, F. M.; Nalamasu, O.; Neenan, T. X. "Chemical amplification mechanisms for microlithography." *Chemistry of Materials* **1991**, *3*, 394-407.

[44] Gu, H. Y.; Zhang, W. Q.; Feng, K. S.; Neckers, D. C. "Photolysis of ((3-trimethylsilyl)propoxy)phenyl) phenyliodonium salts in the presence of 1-naphthol and 1-methoxynaphthalene." *Journal of Organic Chemistry* **2000**, *65*, 3484-3488.

[45] Gu, H. Y.; Ren, K. T.; Grinevich, O.; Malpert, J. H.; Neckers, D. C. "Characterization of iodonium salts differing in the anion." *Journal of Organic Chemistry* **2001**, *66*, 4161-4164.

[46] Narayanan, J.; Deotare, V. W.; Bandyopadhyay, R.; Sood, A. K. "Gelation of aqueous pectin solutions: A dynamic light scattering study." *Journal of Colloid and Interface Science* **2002**, *245*, 267-273.

[47] Fang, Y. P.; Al-Assaf, S.; Phillips, G. O.; Nishinari, K.; Funami, T.; Williams, P. A.; Li, L. B. "Multiple steps and critical behaviors of the binding of calcium to alginate." *Journal of Physical Chemistry B* **2007**, *111*, 2456-2462.

[48] Poncelet, D.; Babak, V.; Dulieu, C.; Picot, A. "A physico-chemical approach to production of alginate beads by emulsification-internal ionotropic gelation."

Colloids and Surfaces a-Physicochemical and Engineering Aspects **1999**, *155*, 171-176.

[49] Zawko, S. A.; Schmidt, C. E. "Simple benchtop patterning of hydrogel grids for living cell microarrays." *Lab on a Chip* **2010**, *10*, 379-383.

[50] Bracher, P. J.; Gupta, M.; Mack, E. T.; Whitesides, G. M. "Heterogeneous Films of Ionotropic Hydrogels Fabricated from Delivery Templates of Patterned Paper." *Acs Applied Materials & Interfaces* **2009**, *1*, 1807-1812.

[51] Raghavan, S. R.; Cipriano, B. H. Gel formation: Phase diagrams using tabletop rheology and calorimetry. In *Molecular Gels*; Weiss, R. G., Terech, P., Eds.; Springer: Dordrecht, 2005; pp 233-244.

[52] Macosko, C. W. *Rheology: Principles, measurements and applications.*; VCH Publishers: New York, 1994.

[53] Sugar and Sweeteners Yearbook tables, Table 3 and 4 ヤ *USDA Economic Research Service*, Table 3 and 4.

[54] Marshall, R. O.; Kooi, E. R. "ENZYMATIC CONVERSION OF D-GLUCOSE TO D-FRUCTOSE." *Science* **1957**, *125*, 648-649.

[55] Bhosale, S. H.; Rao, M. B.; Deshpande, V. V. "Molecular and industrial aspects of glucose isomerase." *Microbiological Reviews* **1996**, *60*, 280-+.

[56] Hanover, L. M.; White, J. S. "MANUFACTURING, COMPOSITION, AND APPLICATIONS OF FRUCTOSE." *American Journal of Clinical Nutrition* **1993**, *58*, S724-S732.

[57] Marriott, B. P.; Cole, N.; Lee, E. "National Estimates of Dietary Fructose Intake Increased from 1977 to 2004 in the United States." *Journal of Nutrition* **2009**, *139*, S1228-S1235.

[58] White, J. S. "Straight talk about high-fructose corn syrup: what it is and what it ain't." *American Journal of Clinical Nutrition* **2008**, *88*, 1716S-1721S.

[59] Bray, G. A.; Nielsen, S. J.; Popkin, B. M. "Consumption of high-fructose corn syrup in beverages may play a role in the epidemic of obesity." *American Journal of Clinical Nutrition* **2004**, *79*, 537-543.

[60] Tappy, L.; Le, K. A. "Metabolic Effects of Fructose and the Worldwide Increase in Obesity." *Physiological Reviews* **2010**, *90*, 23-46.

[61] Johnson, R. J.; Segal, M. S.; Sautin, Y.; Nakagawa, T.; Feig, D. I.; Kang, D. H.; Gersch, M. S.; Benner, S.; Sanchez-Lozada, L. G. "Potential role of sugar

(fructose) in the epidemic of hypertension, obesity and the metabolic syndrome, diabetes, kidney disease, and cardiovascular diseased." *American Journal of Clinical Nutrition* **2007**, *86*, 899-906.

[62] Moeller, S. M.; Fryhofer, S. A.; Osbahr, A. J.; Robinowitz, C. B.; Amer Med, A. "The Effects of High Fructose Syrup." *Journal of the American College of Nutrition* **2009**, *28*, 619-626.

[63] Borra, S. "Consumer perspectives on food labels." *American Journal of Clinical Nutrition* **2006**, *83*, 1235S-1235S.

[64] Heller, A.; Feldman, B. "Electrochemical glucose sensors and their applications in diabetes management." *Chemical Reviews* **2008**, *108*, 2482-2505.

[65] Raba, J.; Mottola, H. A. "GLUCOSE-OXIDASE AS AN ANALYTICAL REAGENT." *Critical Reviews in Analytical Chemistry* **1995**, *25*, 1-42.

[66] Vashist, S. K.; Zheng, D.; Al-Rubeaan, K.; Luong, J. H. T.; Sheu, F. S. "Technology behind commercial devices for blood glucose monitoring in diabetes management: A review." *Analytica Chimica Acta* **2011**, *703*, 124-136.

[67] Wu, Q.; Wang, L.; Yu, H. J.; Wang, J. J.; Chen, Z. F. "Organization of Glucose-Responsive Systems and Their Properties." *Chemical Reviews* **2011**, *111*, 7855-7875.

[68] Newman, J. D.; Turner, A. P. F. "Home blood glucose biosensors: a commercial perspective." *Biosensors & Bioelectronics* **2005**, *20*, 2435-2453.

[69] Heller, A.; Feldman, B. "Electrochemistry in Diabetes Management." *Accounts of Chemical Research* **2010**, *43*, 963-973.

[70] Meyer, W. L.; Liu, Y.; Shi, X. W.; Yang, X. H.; Bentley, W. E.; Payne, G. F. "Chitosan-Coated Wires: Conferring Electrical Properties to Chitosan Fibers." *Biomacromolecules* **2009**, *10*, 858-864.

[71] Wang, J. "Electrochemical glucose biosensors." *Chemical Reviews* **2008**, *108*, 814-825.

[72] Johnson, L. M.; DeForest, C. A.; Pendurti, A.; Anseth, K. S.; Bowman, C. N. "Formation of Three-Dimensional Hydrogel Multilayers Using Enzyme-Mediated Redox Chain Initiation." *Acs Applied Materials & Interfaces* **2010**, *2*, 1963-1972.

[73] Ikeda, M.; Tanida, T.; Yoshii, T.; Hamachi, I. "Rational Molecular Design of Stimulus-Responsive Supramolecular Hydrogels Based on Dipeptides." *Advanced Materials* **2011**, *23*, 2819-+.

[74] Wang, C. Y.; Liu, H. X.; Gao, Q. X.; Liu, X. X.; Tong, Z. "Alginate-calcium carbonate porous microparticle hybrid hydrogels with versatile drug loading capabilities and variable mechanical strengths." *Carbohydrate Polymers* **2008**, *71*, 476-480.

[75] Astete, C. E.; Sabliov, C. M.; Watanabe, F.; Biris, A. "Ca2+ Cross-Linked Alginic Acid Nanoparticles for Solubilization of Lipophilic Natural Colorants." *Journal of Agricultural and Food Chemistry* **2009**, *57*, 7505-7512.

[76] Lee, K. Y.; Mooney, D. J. "Alginate: Properties and biomedical applications." *Progress in Polymer Science* **2012**, *37*, 106-126.

[77] Cheng, Y.; Luo, X. L.; Betz, J.; Payne, G. F.; Bentley, W. E.; Rubloff, G. W. "Mechanism of anodic electrodeposition of calcium alginate." *Soft Matter* **2011**, *7*, 5677-5684.

[78] Javvaji, V.; Baradwaj, A. G.; Payne, G. F.; Raghavan, S. R. "Light-Activated Ionic Gelation of Common Biopolymers." *Langmuir* **2011**, *27*, 12591-12596.

[79] Stokke, B. T.; Draget, K. I.; Smidsrod, O.; Yuguchi, Y.; Urakawa, H.; Kajiwara, K. "Small-angle X-ray scattering and rheological characterization of alginate gels. 1. Ca-alginate gels." *Macromolecules* **2000**, *33*, 1853-1863.

[80] Ventura, E. E.; Davis, J. N.; Goran, M. I. "Sugar Content of Popular Sweetened Beverages Based on Objective Laboratory Analysis: Focus on Fructose Content." *Obesity* **2011**, *19*, 868-874.

[81] Thornton, P. D.; Mart, R. J.; Webb, S. J.; Ulijn, R. V. "Enzyme-responsive hydrogel particles for the controlled release of proteins: designing peptide actuators to match payload." *Soft Matter* **2008**, *4*, 821-827.

[82] Thornton, P. D.; Mart, R. J.; Ulijn, R. V. "Enzyme-responsive polymer hydrogel particles for controlled release." *Advanced Materials* **2007**, *19*, 1252-+.

[83] Yang, Z.; Liang, G.; Xu, B. "Enzymatic hydrogelation of small molecules." *Accounts of Chemical Research* **2008**, *41*, 315-326.

[84] Berron, B. J.; Johnson, L. M.; Ba, X.; McCall, J. D.; Alvey, N. J.; Anseth, K. S.; Bowman, C. N. "Glucose Oxidase-Mediated Polymerization as a Platform for Dual-Mode Signal Amplification and Biodetection." *Biotechnology and Bioengineering* **2011**, *108*, 1521-1528.

[85] Palsson, B. O.; Bhatia, S. N. *Tissue Engineering*; Pearson Prentice Hall, 2004.

[86] Whitesides, G. M.; Grzybowski, B. "Self-assembly at all scales." *Science* **2002**, *295*, 2418-2421.

[87] Langer, R.; Vacanti, J. P. "TISSUE ENGINEERING." *Science* **1993**, *260*, 920-926.

[88] Taguchi, T. "Assembly of cells and vesicles for organ engineering." *Science and Technology of Advanced Materials* **2011**, *12*.

[89] Hennink, W. E.; van Nostrum, C. F. "Novel crosslinking methods to design hydrogels." *Advanced Drug Delivery Reviews* **2002**, *54*, 13-36.

[90] Payne, G. F.; Kim, E.; Cheng, Y.; Wu, H.-C.; Ghodssi, R.; Rubloff, G. W.; Raghavan, S. R.; Culver, J. N.; Bentley, W. E. "Accessing biology's toolbox for the mesoscale biofabrication of soft matter." *Soft Matter* **2013**, *9*, 6019-6032.

[91] Dowling, M. B.; Kumar, R.; Keibler, M. A.; Hess, J. R.; Bochicchio, G. V.; Raghavan, S. R. "A self-assembling hydrophobically modified chitosan capable of reversible hemostatic action." *Biomaterials* **2011**, *32*, 3351-3357.

[92] Bu, H. T.; Kjoniksen, A. L.; Knudsen, K. D.; Nystrom, B. "Effects of surfactant and temperature on rheological and structural properties of semidilute aqueous solutions of unmodified and hydrophobically modified alginate." *Langmuir* **2005**, *21*, 10923-10930.